Article:
Zhu, K, Mao, G, Wu, D et al. (7 more authors) (2020) Highly Branched RG-I Domain Enrichment Is Indispensable for Pectin Mitigating against High-Fat Diet-Induced Obesity. Journal of Agricultural and Food Chemistry, 68 (32). pp. 8688-8701. ISSN 0021-8561

https://doi.org/10.1021/acs.jafc.0c02654

Highly Branched RG-I Domain Enrichment are Indispensable for Pectin Mitigating Against High-Fat Diet-Induced Obesity

Kai Zhu[1], Guizhu Mao[1], Dongmei Wu[1], Chengxiao Yu[1], Hang Xiao[1,6], Xingqian Ye[1, 2, 3], Robert J. Linhardt[4], Caroline Orfila[5], Shiguo Chen[1, 2, 3]*

[1] College of Biosystems Engineering and Food Science, National-Local Joint Engineering Laboratory of Intelligent Food Technology and Equipment, Zhejiang Key Laboratory for Agro-Food Processing Integrated Research Base of Southern Fruit and Vegetable Preservation Technology, Zhejiang International Scientific and Technological Cooperation Base of Health Food Manufacturing and Quality Control, Zhejiang University, Hangzhou 310058

[2] Fuli Institute of Food Science, Zhejiang University, Hangzhou 310058

[3] Ningbo Research Institute, Zhejiang University, Ningbo 315100

[4] Center for Biotechnology and Interdisciplinary Studies, Rensselaer Polytechnic Institute, Troy, New York 12180, USA

[5] School of Food Science and Nutrition, University of Leeds, Leeds LS2 9JT, United Kingdom

[6] Department of Food Science, University of Massachusetts, Amherst, MA 01003, U.S.A.

*** Correspondence:**

Shiguo Chen

chenshiguo210@163.com

Keywords: RG-I, Molecular weight, Side chain, Pectin, High-fat diet, Obesity, Gut microbiota

Abstract

Obesity is associated with gut microbiome dysbiosis. Our previous research has shown that highly branched RG-I enriched pectin (WRP, 531.5 kDa, 70.44% RG-I, Rha:(Gal+Ara)=20) and its oligosaccharide with less branched (DWRP, 12.1 kDa, 50.29% RG-I, Rha:(Gal+Ara)=6) are potential prebiotics. The present study is conducted to uncover the impact by which the content, molecular size and branch degrees of RG-I on the inhibiting effect of high-fat diet (HFD)-induced obesity. The commercial pectin (CP, 496.2 kDa, 35.77% RG-I, Rha:(Gal+Ara)=6), WRP and DWRP were orally administered to HFD-fed C57BL/6J mice (100mg kg^{-1} d^{-1}) to determine their individual effects on obesity. WRP significantly prevented bodyweight gain, insulin resistance, and inflammatory responses in HFD-fed mice. No obvious anti-obesity effect was observed in either CP or DWRP supplementation. Mechanistic study revealed that CP and DWRP could not enhance the diversity of gut microbiota, while WRP treatment positively modulated the gut microbiota of obese mice by increasing the abundance of *Butyrivibrio*, *Roseburia*, *Barnesiella*, *Flavonifractor, Acetivibrio*, and *Clostridium* cluster IV. Furthermore, the WRP significantly promoted browning of white adipose tissue in HFD-fed mice, while CP and DWRP did not. WRP can attenuate the HFD-induced obesity by modulation of gut microbiota and lipid metabolism. Highly branched RG-I domain enrichment are essential for pectin mitigating against the HFD-induced obesity.

51 **Graphical abstract:**

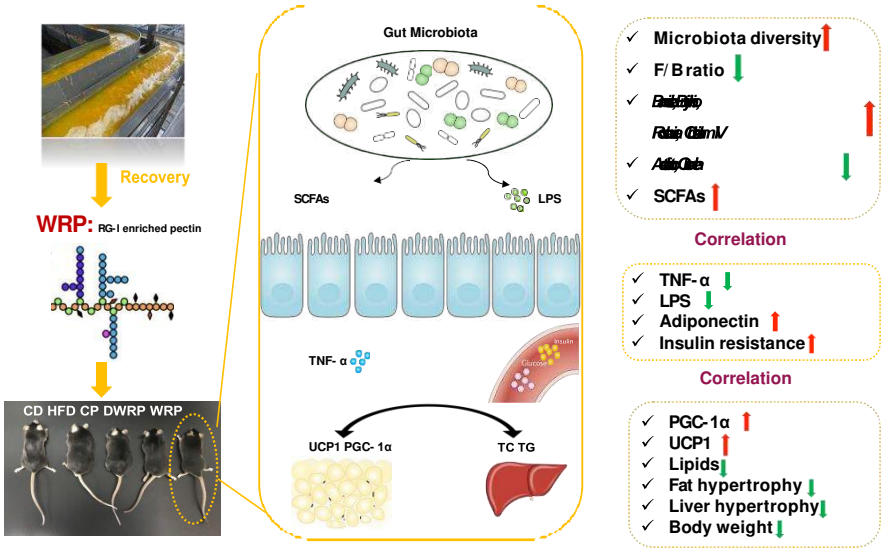

52

53 **Introduction**

54 The prevention of obesity is a challenge of global proposition. Evidence has shown
55 that obesity is associated with reduced gut bacterial diversity or altered proportions of
56 bacterial species [1-4]. Consumption of plant polysaccharides revealed a significant and
57 positive effect on adiposity-induced lipid metabolic disorders and gut microbiota
58 dysbiosis [5-8]. Among them, pectin and derived-oligosaccharides are good candidate
59 modulators of obesity due to their fermentation potential by various probiotic
60 microorganisms to modulate the obesity due to their complex structure that fermented
61 by various of probiotics [9-11].

62 Pectin is a complex heteropolysaccharide which consists of structurally distinct
63 domains including homogalacturonan (HG), xylogalacturonan (XGA),
64 rhamnogalacturonan type I (RG-I), rhamnogalacturonan type II (RG-II), arabinan, and
65 arabinogalactan. RG-I is comprised of a backbone being formed from a repeating

66 disaccharide of [→2)-α-L-Rha*p*-(1→4)-α-D-GalA*p*-(1→] residues with Ara and Gal
67 residues attached to the *O*-4 or *O*-3 position of α-L-Rha*p* backbone units [12]. It is usually
68 removed from commercial pectin preparations by hot acid treatment as it is considered
69 a hinder for pectin gelling. However, accumulating evidence has illustrated that pectin
70 containing RG-I regions from various sources can modulate the composition of obesity-
71 related intestinal microbiota and increase the production of butyrate, which is a
72 dominant protective agent against obesity [13-17]. Recent findings suggested has been
73 reported that polysaccharide utilization loci (PULs) of gut bacteria activated by
74 different RG-I domains can recruit a myriad of glycoside hydrolases (GHs) and
75 polysaccharides lyases (PLs) for metabolism of RG-I pectin molecules [18-19]. Thus, RG-I
76 is hypothesized to contribute significantly to bacterial fermentation in the colon leading
77 to favorable changes in gut microbiota composition [20-21]. Particularly, Khodaei and his
78 colleagues have confirmed that potato RG-I pectin stimulated the growth of
79 *Lactobacillus spp.* and *Bifidobacterium spp*. Reduction in these two species are
80 proposed biomarker of gut dysbiosis and found to be decreased under high-fat diet
81 (HFD) conditions [22]. A recent research also indicated the pectin containing RG-I can
82 modulate the composition of obesity-related gut microbiota and upregulate the
83 production of butyrate—a dominant protective agent against obesity [23]. Moreover,
84 apple pectin rich in RG-I strongly promoted *Bifidobacterium*, *Bacteroides*, and
85 *Lactobacillus* in HFD-fed mice colon, subsequently producing short-chain fatty acids
86 (SCFAs) which limits the secretion of proinflammatory cytokines and alleviated the

87 obesity caused inflammation [24]. However, up to now the impact of RG-I content in
88 pectin on the HFD-induced obesity is still unclear.

89 Apart from the RG-I content, another factor affected the bioactivity of the RG-I
90 pectin is molecular size [25]. A recent study on citrus pectic oligosaccharides containing
91 RG-I with a molecular weight of 3~4 kDa have shown hypocholesterolemic effects on
92 HFD-fed mice by modulating specific gut bacterial groups [10]. Besisdes, the report from
93 Gómez et al. has shown pectic oligosaccharides (5.9~22.8 kDa) containing relative high
94 content RG-I (37.65%) caused better shifts prebiotic properties than high Mw pectin
95 (51.4~82 kDa), confirming the essential of molecular size in functional properties of
96 RG-I pectin [26]. However, most of the research merely focused on the preparation and
97 probiotic effect of pectic oligosaccharides primarily consists of HG, less studies were
98 conducted on RG-I enriched oligosaccharides [11, 26-27]. Furthermore, a greater proportion
99 of side chains in RG-I pectin was confirmed that can promote the growth of *Bacteroides*
100 species [28-30]. The arabino/galacto-oligosaccharides derived from the side chains of RG-I
101 were proved to be more fermented by *Bifidobacterium* than those from backbone of
102 RG-I [22]. These observations indicate that the neutral sugar branching chains may have
103 a great impact on the gut microbial composition improvement of RG-I enriched
104 oligosaccharides. Since the neutral sugar side chains were degraded significantly during
105 the pectic oligosaccharide preparation process. There is also necessary to take the
106 branching degrees into account for assessment the RG-I oligosaccharides' beneficial
107 effects in the gut microbiota.

108 In our previous study, RG-I enriched oligosaccharides (DWRP, 50.29% RG-I
109 content, 12.1 kDa, Rha: (Gal+Ara)=1:6) degraded from citrus canning processing basic
110 water recovered pectin (WRP, 70.44% RG-I, 531.5 kDa, Rha: (Gal+Ara)=1:20) were
111 obtained by metal-free Fenton reaction. DWRP can significantly enriched
112 *Bifidobacterium and Lactobacillus* populations, and WRP can improve the *Bacteroides*,
113 *Desulfovibrio* and Ruminococcaceae in mice [29]. The results evidenced both the highly
114 branched RG-I enriched pectin with large Mw and RG-I oligosaccharides with less
115 branching degree can modulate the gut microbiota. However, these effects on gut
116 microbe of obesity mouse is still unclear.

117 Therefore, the main aim of this study was to uncover the contribution by which
118 RG-I content, molecular size and branching degrees of pectin to the alleviation of HFD-
119 induced obesity and obesity-induce microbiota dysbiosis shaping. The RG-I enriched
120 pectin recovered (WRP), its degradation products (DWRP) and commercial HG
121 dominated pectin (CP, 496.2 kDa, 35.77% RG-I, Rha:(Gal+Ara)=6) were selected in
122 this study. First, investigating the effects of CP, WRP, and DWRP treatment on obesity
123 and obesity-induced metabolic disorders in HFD-fed mice. Then, the contribution of
124 pectin on gut microbiota composition and SCFAs were studied by 16S rRNA and gas
125 chromatography (GC). Moreover, qRT-PCR analysis and immunohistochemistry were
126 also used to analyze the expression of genes and proteins related to brown-like
127 adipocyte formation, respectively.

128 2. Experimental Section

129 2.1 Preparation of Pectin

130 Rhamnogalacturonan-I (RG-I)-enriched pectin (WRP) and its degradation
131 products (DWRP) was recovered from citrus (*Citrus unshiu Marc.*) processing water
132 by sequential acid and alkaline treatments in a previous study [31]. WRP (Mw=531.5 kDa)
133 was recovered from the citrus segments material and was previously reported to have
134 70.44% of RG-I content with high degree of side chain branching (Rha:
135 (Gal+Ara)=1:20), while its depolymerized fraction DWRP (Mw=12.1 kDa, 56.29%
136 RG-I content) with less side chain branching (Rha: (Gal+Ara)=1:6). Commercial pectin
137 (CP) was bought from Sigma-Aldrich (Shanghai, China). and is mainly composed of
138 HG (52.55%) with an average Mw of 496.2 kDa and low degree of side chain branching
139 (Rha: (Gal+Ara)=1:6) was used in the present study.

140 2.2 Animal Experiments

141 Fifty C57BL/6J male mice (SPF, 6-8 weeks old, IACUC-20180917-02) were kept
142 under specific-pathogen-free conditions in a 12-hour light/dark cycle with free access
143 to standard chow diet (CD; 12% of energy from fat; Rodent diet, SHOBREE, Jiangsu
144 Synergy Pharmaceutical Biological Engineering Co, Ltd, Nanjing China) and sterile
145 drinking water in a temperature-controlled room (21 °C±2 °C). After an
146 accommodation period of 1 week, the mice were randomly divided into five groups (10
147 mice/group) and were fed for 8 weeks with CD, high fat diet (HFD, 60% of energy
148 from fat; Research Diets D12492, Opensource Diets, USA), HFD with 100mg/kg CP
149 (HFD-CP), HFD with 100mg/kg WRP (HFD-WRP), HFD with 100mg/kg DWRP
150 (HFD-DWRP). A certain amount of pectin according to the dosages of 100mg/kg was

151 dissolved in 200 μL distilled water and administrated orally via intragastric gavage once
152 per day. The compositions and energy densities of the diets are listed in **Table S1**. Body
153 weight and food intake were measured weekly.

154 The oral glucose tolerance test (OGTT) was performed three days before sacrifice.
155 Overnight-fasted mice were administrated with glucose solution (2 g/kg body weight,
156 66% solution) by oral gavage, then blood glucose was measured from tail vein blood at
157 0, 30, 60, 90, 120 min using test strips (ACCU-CHEK Performa) and a portable glucose
158 meter (Roche Diagnostics, Shanghai, China). The blood glucose level before glucose
159 administration represented the fasting glucose concentration. Incremental area under
160 the curve (AUC) was calculated using the trapezoidal method.

161 Mice were fasting for 12 hours, anaesthetised and sacrificed by cervical
162 dislocation after 9 weeks. Blood and tissues were collected and stored at -80 °C until
163 further use. All procedures were approved by the Institutional Animal Care and Use
164 Committee of Zhejiang University School of Medicine.

165 2.3 Biochemical analysis and cytokine measurements of serum

166 Serum was isolated by centrifugation (4 °C, 12,000g, 10 min). Serum total
167 cholesterol (TC), triglycerides (TG), high density lipoprotein cholesterol (HDL-C) and
168 low density lipoprotein cholesterol (LDL-C) were measured using commercial kits
169 (Nanjing Jiancheng Bioengineering Institute, Nanjing, China) according to the
170 manufacturer's instructions. Serum TNF-α, IL-6, LPS, Insulin and adiponectin protein
171 levels were then quantified using commercial ELISA kits (Cloud-clone Crop, USA)

172 following the manufacturer's instruction.

173 **2.4 Liver and epididymal fat histology**

174 The fresh liver, inguinal white adipose tissue (iWAT) and epididymis WAT
175 (eWAT) were isolated and fixed with 4% neutral formalin solution at room temperature
176 for 48 h. After dehydration, eWAT, iWAT and liver were clarified in benzene and
177 embedded in low melting point paraffin wax. Sections (3 nm thick) were cut and stained
178 with haematoxylin and eosin (H&E staining) for light microscopic examination. All of
179 these assays were performed in a blinded manner.

180 **2.5 Immunohistochemistry staining**

181 The paraffin sections of iWAT were subjected to deparaffination, antigen retrieval,
182 endogenous peroxidase activity blocking. Thereafter, slides were incubated with UCP1
183 primary antibody (Santacruz Biotechnology Inc., USA) and horseradish peroxidase
184 (HRP)-conjugated secondary antibody. After 3, 3-diaminobenzidine (DAB)
185 immunostaining, harris hematoxylin counterstaining, dehydration and coverslipping,
186 the sections were observed in DS-Ri1-U3 Nikon digital imaging system and the positive
187 integral optical density (IOD) of UCP1 in the immunohistochemical pictures was
188 analyzed with the Image J software (National Institute of Health, MD, USA).

189 **2.6 RNA extraction and quantitative real-time PCR analysis**

190 Total RNA was extracted from eWAT, iWAT, and BAT using TRIzol reagent
191 (Invitrogen, CA, USA), which was then used to synthesize cDNA with PrimeScript RT
192 reagent Kit with gDNA Eraser (Takara, Beijing, China). Quantitative real-time PCR
193 was performed using SYBR Green Master Mix (Applied biosystems, CA, USA), 96-

194 well plates and an Applied Biosystems QuantStudio 3 Real-Time PCR instrument (Life
195 Technologies, Singapore). qPCR was performed for 40 cycles with following programs:
196 50 °C for 2 min, 95 °C for 1s, 60 °C for 40s. Relative quantification was done based on
197 the $2^{-\Delta\Delta CT}$ method. Expression was normalized to the housekeeping gene.

198 2.7 16S rRNA gene analysis

199 Cecal samples were collected and used for the bacterial 16S rRNA sequencing.
200 Five samples of each group were selected randomly for 16S rRNA analysis. DNA was
201 extracted from the cecal solid contents of mice by using the E.Z.N.A. ®Stool DNA Kit
202 (D4015, Omega, Inc., USA) according to manufacturer's instructions. The total DNA
203 was eluted in 50 μL of Elution buffer and stored at -80 °C until measurement in the
204 PCR by LC-Bio Technology Co., Ltd.The V3-V4 region of the prokaryotic (bacterial
205 and archaeal) small-subunit (16S) rRNA gene was amplified with slightly modified
206 versions of primers 338F (5'-ACTCCTACGGGAGCAGCAG-3') and 806R (5'-
207 GGACTACHVGGGTWTCTAAT-3') [32]. The 5' ends of the primers were tagged with
208 specific barcods per sample and sequencing universal primers.

209 The PCR products were purified by AMPure XT beads (Beckman Coulter
210 Genomics, Danvers, MA, USA) and quantified by Qubit (Invitrogen, USA). The
211 amplicon pools were prepared for sequencing and the size and quantity of the amplicon
212 library were assessed on Agilent 2100 Bioanalyzer (Agilent, USA) and with the Library
213 Quantification Kit for Illumina (Kapa Biosciences, Woburn, MA, USA), respectively.
214 PhiX Control library (v3) (Illumina) was combined with the amplicon library (expected

215 at 30%). The libraries were sequenced either on 300PE MiSeq runs and one library was
216 sequenced with both protocols using the standard Illumina sequencing primers,
217 eliminating the need for a third (or fourth) index read.

218 Samples were sequenced on an Illumina MiSeq platform according to the
219 manufacturer's recommendations, provided by LC-Bio. Paired-end reads was assigned
220 to samples based on their unique barcode and truncated by cutting off the barcode and
221 primer sequence. Paired-end reads were merged using FLASH. Quality filtering on the
222 raw tags were performed under specific filtering conditions to obtain the high-quality
223 clean tags according to the FastQC (V 0.10.1). Chimeric sequences were filtered using
224 Verseach software (v2.3.4). Sequences with ≥97% similarity were assigned to the
225 same operational taxonomic units (OTUs) by Verseach (v2.3.4). Representative
226 sequences were chosen for each OTU, and taxonomic data were then assigned to each
227 representative sequence using the RDP (Ribosomal Database Project) classifier. The
228 differences of the dominant species in different groups, multiple sequence alignment
229 was conducted using the PyNAST software to study phylogenetic relationship of
230 different OTUs. OTUs abundance information were normalized using a standard of
231 sequence number corresponding to the sample with the least sequences. Alpha diversity
232 is applied in analyzing complexity of species diversity for a sample through 4 indices,
233 including Chao1, Shannon, Simpson and Observed species. All indices of samples were
234 calculated with QIIME (Version 1.8.0). Beta diversity analysis was used to evaluate
235 differences of samples in species complexity. Beta diversity were calculated by

236 principle co-ordinates analysis (PCoA) and cluster analysis by QIIME software
237 (Version 1.8.0). The spearman's rho nonparametric correlations between the gut
238 microbiota and heal-related indexes were determined using R packages (V2.15.3).
239 Alpha diversity indexes, relative abundance of phyla, principal component
240 analysis (PCA) and linear discriminant analysis (LDA) effect size (LEFse) analysis
241 were assessed.

242 2.8 Ceacal and colonic short-chain fatty acids

243 Production of SCFA in the ceca and feces of mice was analysed using a 7890A
244 GC (Agilent Technologies, Stockport, UK) using a slightly modified method [6]. Detailed
245 description of these methods is described in a previous study.

246 2.9 Statistical Analysis

247 Data were expressed as means ± SD. Statistical analysis was performed using
248 GraphPad Prism V.7.04 (GraphPad Software, USA). One-way analysis of variance
249 (ANOVA) for multiple comparisons was conducted, followed by the non-parametric
250 Kruskal–Wallis test with Dunnett's multiple comparisons test.[33] Significance was set
251 at $p < 0.05$.

252 3. Results

253 3.1 WRP Prevented Body Weight Gain in HFD-induced Obese Mice

254 To test the effects of pectin supplementation on body weight, we fed mice with
255 HFD with or without pectin supplementation for 8 weeks. Compared with the CD, mice
256 fed an HFD showed a significant and sustained increase body weight (260%) (**Figure**
257 **1**). Notably, WRP supplementation dramatically prevent the body weight gain caused

258 by HFD ($p < 0.001$, **Figure 1B&C**). However, no significant improvement in weight
259 gain was observed in the HFD-CP and HFD-DWRP groups. As shown in **Figure 1 C~E**,
260 HFD significantly induced the weight gain of liver, kidney, inguinal white adipose
261 tissue and epididymal white adipose tissue of mice. In parallel with weight gain caused
262 by HFD (**Figure 1E**), the weight gain of white adipose tissue and visceral fat of HFD
263 fed mice was prevented decreased observably when intervened by WRP (iWAT, $p <$
264 0.001; eWAt, $p < 0.01$). Besides, WRP apparently reduced macrosteatosis, hepatocyte
265 ballooning in the livers of obese mice. The liver and fat tissue morphology in HFD-CP
266 and HFD-DWRP groups was the same as in the HFD. The fat tissue morphology failed
267 to maintained in HFD-CP and HFD-DWRP group (**Figure 2**).
268 Some reports suggested that fucoidan was reported to affected appetite regulation
269 and subsequent control of body weight [34]. There was no significant difference in food
270 intake between groups (see on **Figure S1**), indicating that the mitigating effects of WRP

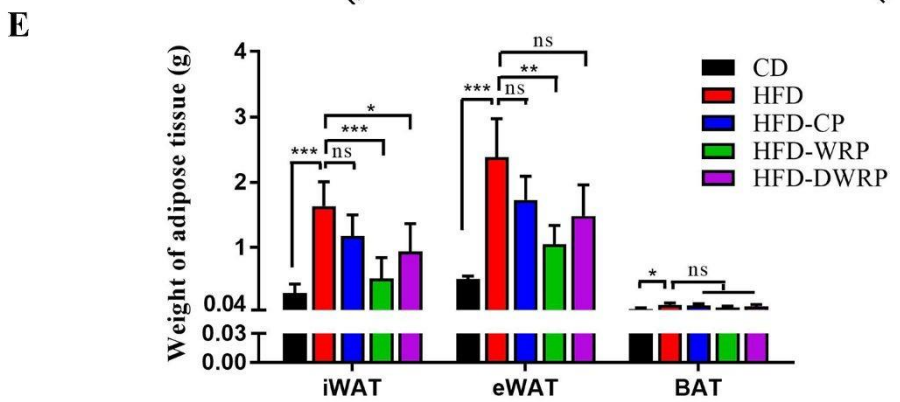

271272

272 **Figure 1.** Whole body and tissue weight fed on conventional chow (CD) and high-fat diet (HFD)
273 for 8 weeks. A: Growth curve of mice in different groups; B : The weight gain of mice in each
274 group after 8 weeks of feeding; C~E: shows the weight of liver, kidney, inguinal white adipose
275 tissue, epididymal white adipose tissue and brown adipose tissue of mice, respectively. (Data are
277 presented as means ± SD (n=8 mice per group). *p < 0.05; **p < 0.01; ***p < 0.001; ****p <
278 0.0001; ns, not significant.

279 3.2 WRP Alleviated HFD-induced Hyperlipidemia, Hyperglycemia, and 280 Inflammatory Responses

281 As shown in **Table 1**, the serum level of total triacylglycerol (TG), total
282 cholesterol (TC), low density lipoprotein cholesterol (LDL-C) and free fatty acids (FFA)

283 in mice were negatively controlled and the high-density lipoprotein cholesterol (HDL-
284 C), adiponectin and HDL-C/LDL-C content positively controlled by WRP treatment.[35]
285 Pro-inflammatory cytokines have been shown systemic inflammation but also insulin
286 resistance [36]. And bacterial lipopolysaccharide (LPS) is an early factor in the triggering
287 of metabolic diseases induced by obesity [37]. The adipose tissues of obese animals and
288 humans secreted considerable level of pro-inflammatory cytokines and LPS compared
289 with lean individuals [36, 38]. In the present study, supplementation of WRP and DWRP
290 significantly controlled the level of serum LPS and TNF-α in HFD-fed mice. Further,
291 to determine the effect of different pectins on glucose homeostasis and insulin
292 sensitivity, OGTT and fasting insulin test were performed. As shown in **Figure 3**, HFD
293 treatment impeded the glucose utilization ability as the levels of fasting blood glucose
294 ($p < 0.0001$) and insulin ($p < 0.01$) were significantly increased compared to CD group.
295 Nevertheless, WPR intervened HFD-fed mice exhibited lower glucose levels at all time
296 points up to 120 min after oral glucose challenge and reduced AUC glycemic response.
297 Moreover, WPR and DWPR supplementation lowered the plasma levels of glucose and
298 insulin compared with the HFD group (**Figure 3D**). Together, WRP effectively
299 alleviated the dyslipidemia of induced by HFD through negatively control of blood
300 lipid and proinflammatory factors content; on the other hand, WRP improved the
301 glucose intolerance and insulin sensitivity.

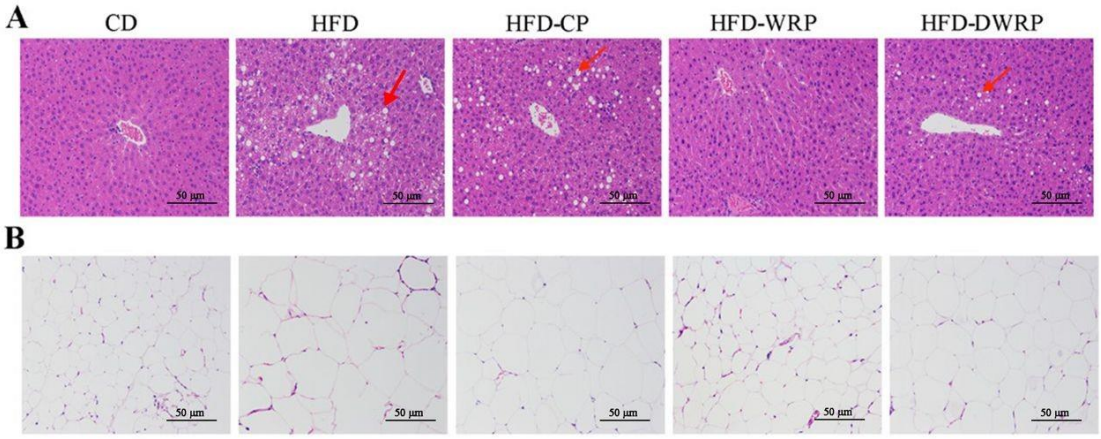

302302

303 **Figure 2.** Histological assessment of livers (A) and epididymal white adipose tissue (B) in HFD-
304 induced obesity mice. (H&E stain, 200×magnification)

305 3.3 WRP Promotes Browning of White Adipocytes in HFD-induced Mice

306 The average cell size of iWAT in HFD group was significant larger than CD group
307 (**Figure 4A**). WRP supplementation the size of iWAT significantly lower than HFD
308 group, but no obvious difference in size of iWAT was observed in both HFD- CP and
309 HFD-DWRP groups. Under some stimulation (cold condition or β-3 adrenergic
310 agonist), the content of mitochondria in WATs increased dramatically and enhances
311 thermogenic properties. This process was called "browning", and brown-like
312 adipocytes expressed large amounts of uncoupling protein 1 (UCP1) to enhance energy
313 expenditure in WATs [39]. As expected, the immunohistochemistry staining results
314 revealed that the expression level of UCP1 protein in iWAT was remarkably
315 upregulated in HFD-WRP group compared to HFD group (**Figure 4A**). Consistent with
316 these changes, qPCR analysis confirmed that WRP increased the mRNA level of UCP1
317 in iWAT (5.65-fold *v.s.* HFD group, $p < 0.001$) (**Figure 4B**). In addition,
318 supplementation of WRP also remarkably increased the expression of some

319 thermogenic genes and beige adipocyte-selective markers in iWAT, such as PRDM16

320 ($p < 0.0001$), PGC-1α ($p < 0.01$), ERRα ($p < 0.05$), mtTFA ($p < 0.05$), Tmem26 ($p <$

321 0.05), CD137 ($p < 0.01$), and Cidea ($p < 0.01$) (**Figure 4B&C**). These findings

322 demonstrated that supplementation of WRP stimulates browning of iWAT and

323 increased adaptive thermogenesis in HFD-fed mice.

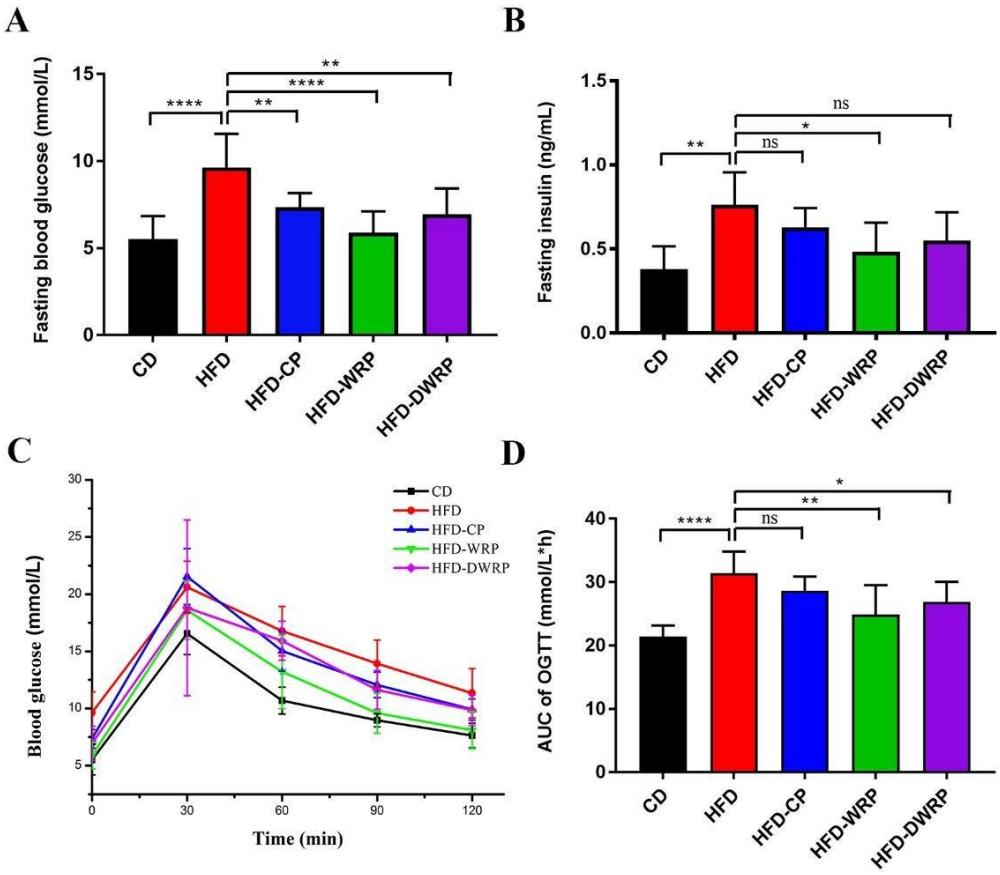

324 324

325 **Figure 3.** Effects of CP, WRP and DWRP on the development of insulin resistance in HFD-fed

326 mice. (A) Fasting blood glucose; (B) fasting insulin; (C) blood glucose; and (D) AUC of OGTT are

327 shown. (*$p < 0.05$; **$p < 0.01$; ***$p < 0.001$; ****$p < 0.0001$; ns, not significant.)

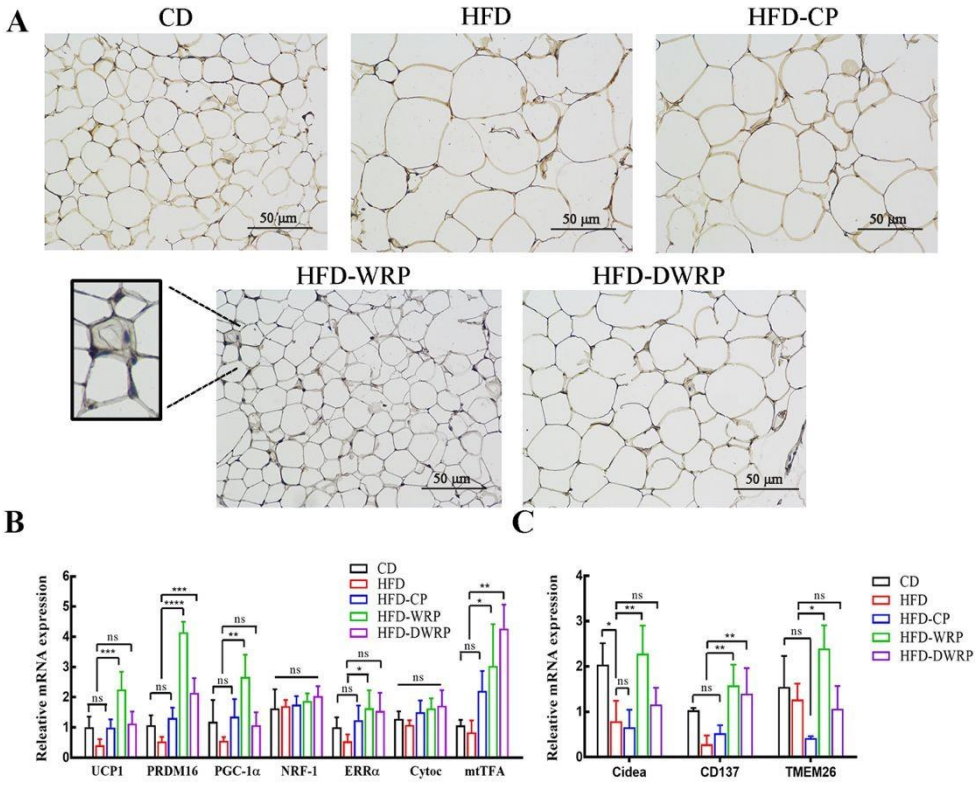

Figure 4. RG-I enriched pectin promoted thermogenesis and browning in iWAT of HFD-fed C57BL/6J mice. (A) Immunohistochemistry for UCP1 protein in iWAT of HFD-fed C57BL/6J mice (magnification 200 times). (B) Thermogenic genes and (C) beige adipocyte-selective markers in iWAT. Relative expression of UCP1, PRDM16, PGC-1α, Nuclear respiratory factor-1 (NRF-1), estrogen-related receptor α (ERRα), Cytochrome c (Cytoc), mitochondrial transcription factor A (mtTFA), Cidea, CD137 and TMEM26 was assessed by qRT-PCR and was Compared to the HFD group. Results are expressed as mean± SD (n ≥ 5). ns, not significant. (*)(**)(***)p < 0.05, 0.01, 0.001, Compared to the HFD group based on one-way analysis of variance (ANOVA) with Duncan's range tests

3.4 WRP Prevents HFD-induced Gut Dysbiosis in Mice

Sequencing analysis of caecal samples from WRP-intervened mice produced an average of 1179±156 observed species compared to the HFD group (960±51) (see on **Table S3**). Next, α-diversity analysis was performed to determine the community richness and diversity. Significant differences in the richness (Chao estimator) and

343 diversity index (Shannon and Simpson index) were detected with the HFD and HFD-
344 WRP groups. In addition, both CP and DWRP shown no remarkable effect on the gut
345 microbiota richness. WRP mitigated the phenomenon of extremely reduced gut
346 microbiota species richness and diversity caused by HFD (see on **Table S3**). The β-
347 diversity analysis based on principal coordinate analysis (PCoA) plots of weighted
348 UniFrac distance and UPGMA showed significant separation was observed between
349 HFD-WRP and HFD groups, and there was also a clear dividing line among the CD,
350 HFD and HFD-WRP groups (**Figure 5A&B**). Collectively, these results indicated that
351 WRP alleviate intensively the gut microbiota dysbiosis in HFD-fed mice compared to
352 CP and DWRP.

353 At the phylum level (**Figure 5C**), HFD markedly increased the
354 Firmicutes/Bacteroidetes (F/B) ratio to 8.78 compared to 1.44 in CD group. WRP
355 supplementation reduced F/B ratio to 1.72 in obese mice which comparable to that of
356 CD group, while HFD-CP and HFD-DWRP groups with a ratio of 8.52 and 6.30
357 respectively (**Figure 5C, Table S4**). The relative abundance of Proteobacteria in HFD-
358 fed mice was significantly higher. Nevertheless, Proteobacteria level showed an
359 inconspicuous decline under the intervention of CP, WRP and DWRP. At class level
360 (**Figure 5D**), the Bacteroidia (Bacteroidetes phylum) comprised 36.27%±14.43%,
361 15.72%±12.05%, 8.83%±4.73%, 23.49%±5.41% and 12.16%±7.12% of gut microbiota
362 in CD, HFD, HFD-CP, HFD-WRP and HFD-DWRP groups. WRP significantly
363 enhanced the abundance of Bacteroidia in the caecum of HFD-fed mice ($p < 0.05$, see

364 on **Table S4**). In contrast, WRP reversed the increase tendency on the abundance of
365 Clostridia (Firmicutes phylum) caused by HFD. Additionally, predominant bacteria in
366 the caecum of mice were Lachnospiraceae (Firmicutes phylum) and
367 Porphyromonadaceae (Bacteroidetes phylum) at family level (see on **Figure S2**). On
368 **Table S4**, the relative abundance of Lachnospiraceae in CD, HFD, and HFD-WRP
369 group were 40.38%±7.23%, 61.98%±8.26%, and 46.42%±7.85%, respectively. On the
370 other side, the relative abundance of Porphyromonadaceae in CD, HFD, and HFD-WRP
371 group were 23.80%±4.64%, 4.14%±1.43%, and 15.92%±6.78%. The results based on
372 the class and family level also explained the decrease of F/B ratio with WRP
373 supplementation. At the genus level, *Un-Lachnospiraceae*, and *Acetatifactor* were
374 predominant bacteria (average relative abundance above 10%), the rest consisted of
375 *Lachnoclostridium, Acetatifactor, Olsenella, Lactobacillus, Butyrivibrio, Alistipes,*
376 *Desulfovibrio,* and *Bacteroides* with an average relative abundance below 5% (**Figure**
377 **5E**). HFD feeding significantly increased the obesity-related bacteria in the cecum of
378 mice, such as *Acetatifactor* and *Olsenella,* while WRP significantly declined the
379 relative abundance of these bacteria (**Figure 4E**, **Table S4**). In addition, the obesity
380 negative-related bacteria (*Barnesiella* and *Butyrivibrio*) were enriched under the
381 intervention of WRP.

382 **Figure 6** shown pathogenic taxa Firmicutes, Clostridia, Clostridiales,
383 Lachospiraceae, *Acetatifactor*. and *Desulfovibrio* were higher in HFD group compared
384 to CD group, while CD group enriched the beneficial phylotypes Bacteroidates,

385 *Bifidobacterium*, *Butyrivibrio*, Porphyromonadaceae, *Alloprevotella*, *Anaerostipes*,
386 and *Anaerotaenia* were enriched in CD group. After treating with CP, there were only
387 2 significant different OUT units. Notably, 19 remarked different OUT units were
388 observed in HFD-WRP group (LDA score threshold > 3 were listed). **Figure 6C**
389 presented the dominate bacteria taxon in the caecum of HFD-fed mice intervened by
390 WRP. Specifically, WRP supplementation significantly increase the abundance of
391 Bacteroidia, *Bacteroidales*, *Barnesiella*, *Butyrivibrio*, *Roseburia*,
392 Prophyromonadaceae, *Flavonifractor, Acetivibrio,* and *Clostridium* cluster IV, while
393 HFD-DWRP group enriched the obesity-related *Butyrivibrio* and *Mucispirillum* genus.
394 The gut dysbiosis induced by HFD was effectively modulated after treatment of WRP,
395 which was due to the more complex RG-I domain stimulating the growth of intestinal
396 microorganisms.
397397

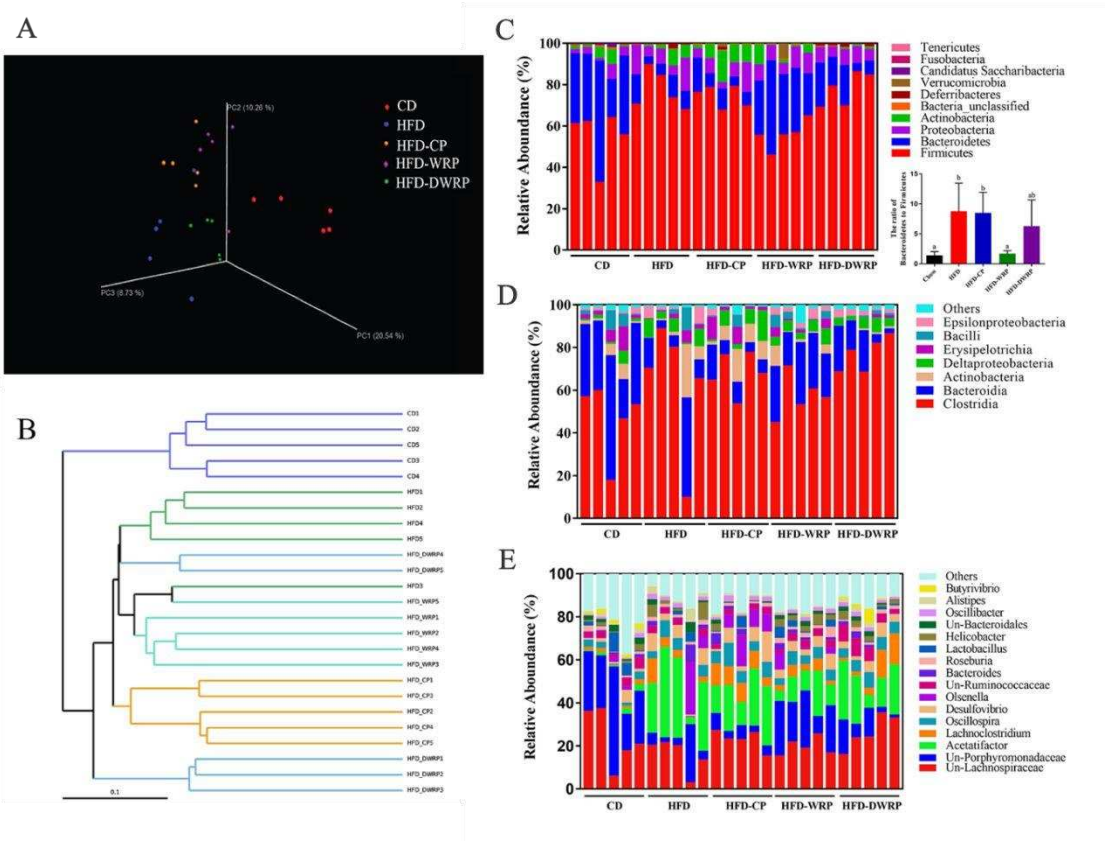

398398

399 **Figure 5.** Structural composition of gut microbiota. (A) PCoA plot of cecal microbiota in HFD-fed

400 mice based on weighted UniFrac metric. (B) UPGMA analysis of cecal microbiota of HFD-fed mice.

401 Cecal microbiota in CD, HFD, HFD-CP, HFD-WRP and HFD-DWRP groups at phylum (C), class

402 (D) and genus (E) level

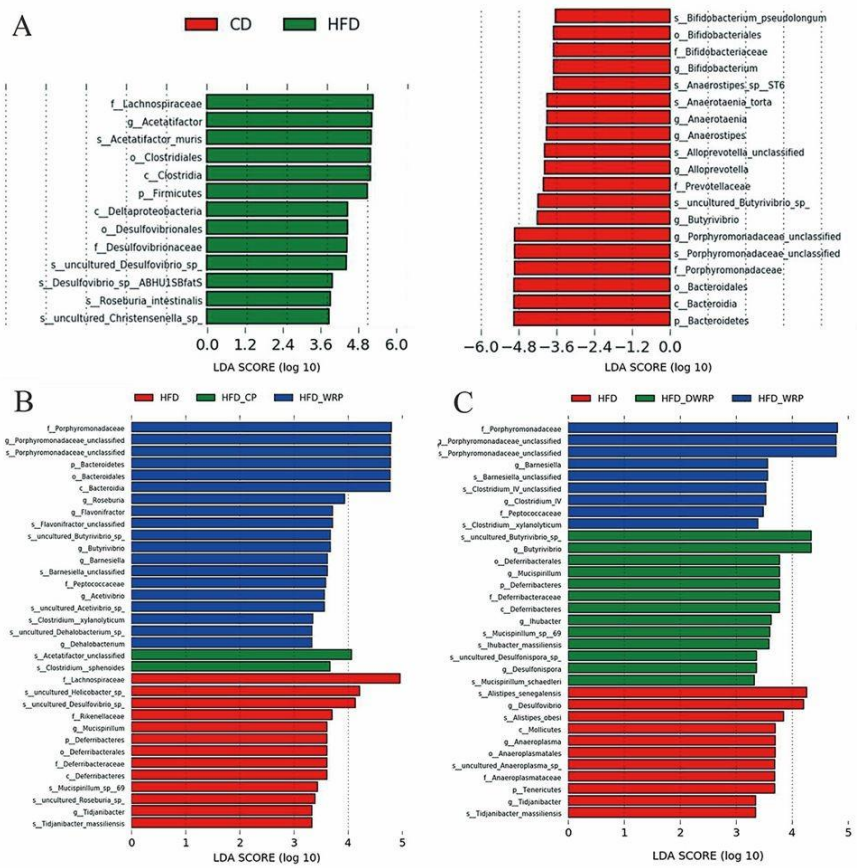

Figure 6. LEfSe comparison of gut microbiota. (A) The LDA score between CD and HFD groups, with LDA score > ±3.6; (B) The LDA score between CD, HFD-WRP and HFD-CP groups, with LDA score > 3.3; (C) The LDA score between CD, HFD-WRP and HFD-DWRP groups, with LDA score > 3.3

3.5 WRP Treatment Promotes Generation of SCFAs in HFD-induce Mice

The gut microbiota was modulated by WRP supplementations in HFD-fed mice, thus, we investigated the effect of WRP on SCFAs-microbial metabolites [40]. HFD significantly inhibited total SCFAs, acetate and propionate in obese mice caecum but had no effect on butyrate generation (**Figure 7**). CP, WRP and DWRP treatment remarkably prevented the suppression of ceacal total SCFAs, acetate and valerate. The

414 of acetate and butyrate, while the production of propionate being promoted by

415 arabinose and glucose fermentation [41]. The increase production of propionate in HFD-

416 WRP and HFD-DWRP may be due to the higher content of arabinose and rhamnose in

417 RG-I pectin compared to CP [20]. Compared with CD group, HFD significantly decreased

418 the acetate, butyrate and valerate levels in the colon feces except propionate. Notably,

419 only HFD-WRP group contained significantly higher concentrations of all kinds of

420 SCFAs in obese mice colon compared to HFD group. However, no significant

421 improvement of these SCFAs was observed in both HFD-CP and HFD-DWRP groups.

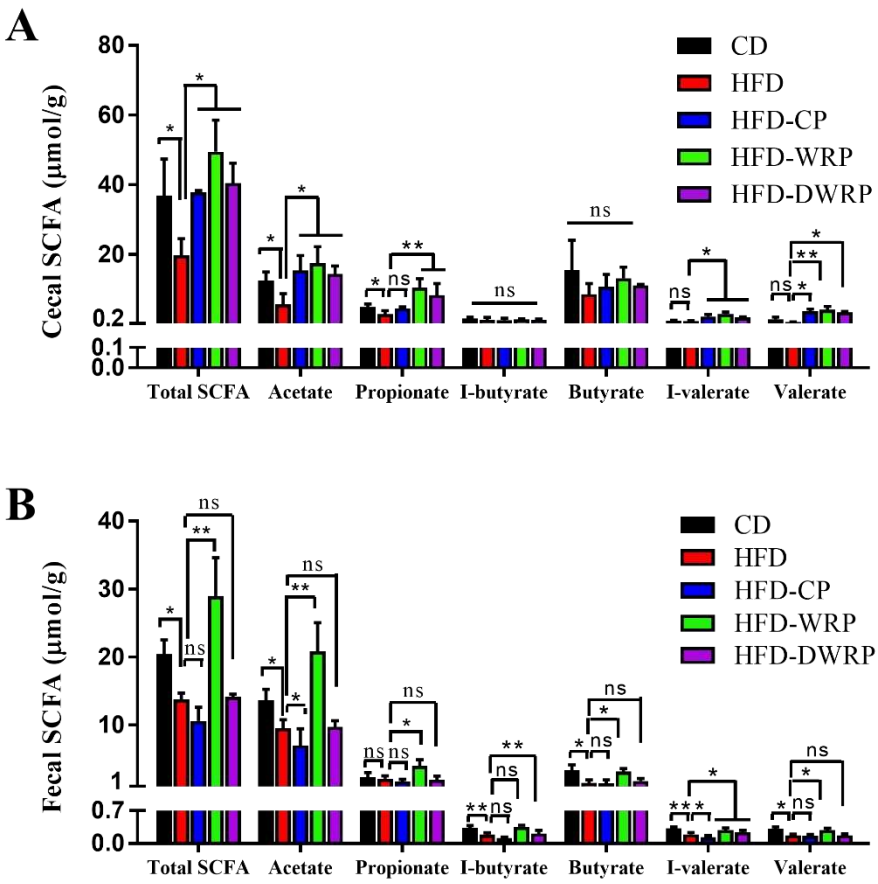

422

423 **Figure 7.** The concentration (μmol/g) of acetic, propionate, butyrate, I-butyrate, valerate, and

424 I-valerate in the cecal contents (A) and colon feces (B) of pectin treated group and chow diet group.

425 **3.6 Correlation of gut microbiota with obesity-related indexes**

426 The Spearman's correlation analysis was performed to clarify the correlation among
427 the microbiota and obesity-related indexes (**Figure 8**). *Pseudoflavonifrator*,
428 *Desulfovibrionaceae*, *Acetatifactor*, *Lachnoclostridium*, and *Robinsoniella* were
429 strongly positively correlated with body weight, epididymal fat weight, TG, TC, and
430 insulin, whereas they were strongly negatively correlated with the gut tissue index ($p <$
431 0.01 or $p < 0.05$), suggesting that they may be the most significant genera for the
432 development of obesity. In addition, the Simpson index, Bifidobacterium,
433 Prorphyromonadaceae, *Acetanaerobacterium*, *Alloprevotella*, *Prevotella*, *Acetivibrio*,
434 *Acetatifactor*, *Prevotella*, *Gemella*, *Eubacterium*, *Ruminococcus*, *Butyrivibrio*, and
435 *Clostridium_sensu_stricto* were highly positively correlated with the gut tissue index,
436 while they were highly negatively correlated with body weight, epididymal fat weight,
437 TG, total cholesterol and LPS ($p < 0.01$ or $p < 0.05$), indicating that they may play the
438 most important role in the obesity.

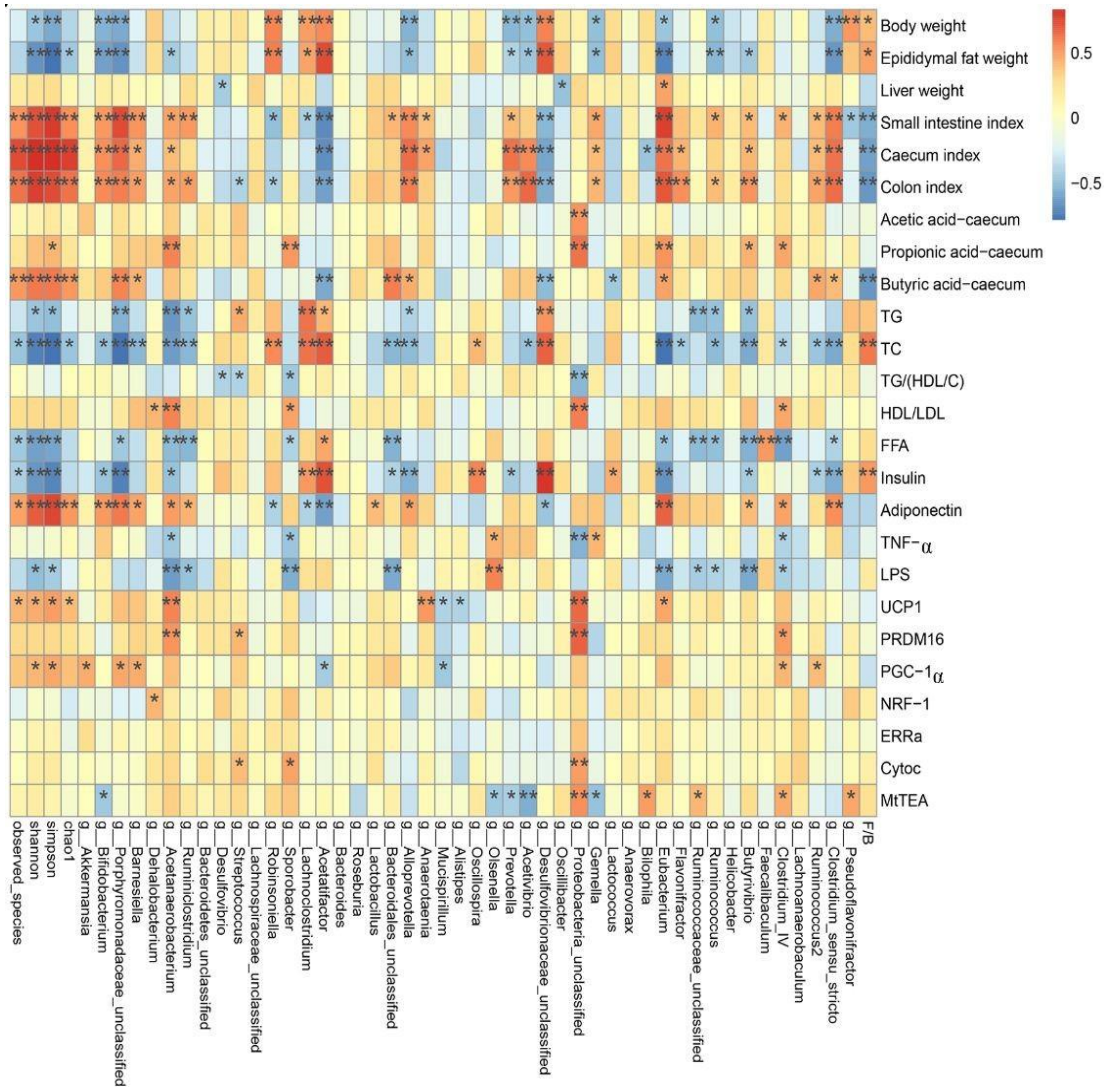

Figure 8. Heatmap of Sperman's correlation between cecal microbiota and health-related indexes. The indexes of α diversity including observed species; the Shannon, Simpson, and Chao1 indexes; The colors range from blue (negative correlation) to red (positive correlation). Significant correlations are marked by $*p < 0.05$ and $**p < 0.01$

4. Discussion

4.1 RG-I Content, Molecular Weight and Branching Chains are Key Factors of Pectin to Prevent Obesity

In our previous research, we found WRP and DWRP had a positive modulation of gut prebiotic microbiota, which stimulated our interests in the potential anti-obesogenic effects of RG-I enriched pectin and its oligosaccharides [29, 31]. However, the gut

450 microbiota of mice changed dramatically under the condition of HFD feeding, and in
451 turn might affect the ferment of pectin in the microbiota. In the present study, we first
452 found that WRP with a high molecular size (531.5 kDa) and RG-I content (70.44%)
453 mitigated against the HFD-induced body weight gain, adipocyte hypertrophy, fatty
454 liver, and hyperlipidemia without suppressing the food intake. On the contrary, no
455 significant decrease in body weight gain was discovered after oral administration of CP
456 (rich in HG domain) and DWRP (depolymerized from WRP). This indicates that the
457 content and molecular structure of RG-I enriched pectin are important for its biological
458 function. Bacterial species characteristic of lean hosts, such as *Butyrivibrio*, *Roseburia*,
459 Prophyromonadaceae, *Barnesiella*, *Flavonifractor*, *Acetivibrio*, and *Clostridium*
460 cluster IV were largely enriched in HFD-WRP group. The anti-obesogenic effects
461 would be explained by the production of SCFAs which could regulate energy
462 homeostasis. Meanwhile, CP and DWRP supplementation barely motivated the
463 enrichment of beneficial bacteria or the diversity of gut microbiota in obese mice.

464 Notably, data published by our group exactly had shown convincingly that CP
465 intervention has not potentially beneficial effect on the gut microbiota of the chow diet
466 feeding mice [29]. We tentatively linked the reason to easy accessibility of pectic
467 backbone (due to less RG-I branches) to microbial degrading enzymes and single
468 monosaccharide composition, which activated much less microbiota species into the
469 fermentation of CP. Multiple species from Bacteroidetes phylum harbored very broad
470 potential to utilize the RG-I domain from pectin [19]. As described by Li el at., RG-I

471 pectin purified from *Fructus Mori* promoted the growth of *Bacteroides*
472 *thetaiotaomicron,* a dominant gut bacteria strain shown to be to beneficial the intestinal
473 mucosa of human [42]. The intricate RG-I pectin comprised complex side-chain
474 components (arabinan, galactan, and arabinogalactan) contributed significantly to the
475 gut microbiota fermentation and favourable changes in microbiota composition [18, 28].
476 Therefore, the high RG-I domain content contributed significantly to the capacity of
477 pectin in HFD-induced obesity modulation.

478 As highlighted by others, pectic oligosaccharides better promoted growth of
479 beneficial bacteria and had the potential to reduce metabolic conditions such as obesity
480 [11, 27, 43]. In here, WRP supplementation mitigated the gut microbiota of HFD-fed mice
481 dramatically. Paradoxically, no modulation effect of gut microbiota was observed in
482 HFD-DWRP group (**Figure. 6**). Specifically, many reports have confirmed that a
483 greater proportion of Ara and Gal in RG-I pectin promoted the growth of *Bacteroides*
484 species [28-30]. Compared to WRP (Rha: (Gal+Ara) ratio of around 1:20), DWRP (Rha:
485 (Gal+Ara)=1:6) had much less degree of Ara and Gla side chains, so large Mw WRP
486 might better regulate the gut microbiota of obese mice [44]. It's also worth noting that the
487 fermentation effect of DWRP in obese mice gut may be different from pectic
488 oligosaccharides which mainly composed of GalA studied in most articles. Concretely,
489 *Barnesiella*, *Clostridium* cluster IV which negatively correlated to obesity were
490 restored in HFD-WRP group, while HFD-DWRP group enriched the *Mucispirillum*
491 genus (**Figure 6**). Since the increased levels of *Mucispirillum* was closely correlated

492 with obesity, which suggested that no anti-obesity effect was observed in HFD-DWRP
493 group may due to the *Mucispirillum* induced gut dysbiosis [45]. This could also give a
494 clue as to why DWRP could not inhibit the HFD-induced body weight gain: the low
495 branching degree structural RG-I domain and low Mw of DWRP led a halfway
496 rectification of gut dysbiosis in obese mice.

497 Our results showed that highly branched RG-I enriched pectin with large
498 molecular size is a strong candidate in prevent of HFD-induced obesity.

499 4.2 WRP alleviates the HFD-induced Obesity via regulation gut dysbiosis and
500 adipocytes thermogenesis

501 In this study, HFD caused an increase in the Firmicutes/Bacteroidetes ratio (F/B),
502 which was reported to be related to obesity [46]. Whereas WRP supplementation reduced
503 the F/B ratio remarkably (**Table 1**, **Figure 5**), since the capacity to utilize RG-I was
504 widespread among colonic Bacteroidetes but relatively uncommon among Firmicutes
505 [20]. Furthermore, we observed changes in the level of Lachospiraceae, *Acetatifactor*,
506 *Desulfovibrio*, *Olsenella*, *Alistipes*, *Mucispirillum* were higher in HFD group.
507 Bacteroidales, *Butyrivibrio*, *Roseburia*, Prophyromonadaceae, *Barnesiella*,
508 *Flavonifractor*, *Acetivibrio*, and *Clostridium* cluster IV, which were restored with WRP
509 supplementation. With regard to the Firmicutes phylum, HFD produced an increase in
510 Lachnospiraceae, which is a potent Firmicutes family related to the regulation of
511 immune and obesity [47]. Here, we observed changes in the level of Lachospiraceae was
512 significant higher in HFD group, but HFD-WRP group presented lower level of
513 Lachnospiraceae. At a genus level, WRP supplementation presented a decrease in

514 *Acetatifactor* which was significantly increased by HFD. As described by several
515 authors, *Acetatifactor* was found abundant in the intestine of obese mouse and has been
516 related to arthritis progression in mice [1, 48-49]. Specially, key members of luminal
517 *Clostridium* cluster IV were known to be butyrate producers, which are closely
518 associated with both obesity and weight loss clearly [50-51]. The presence *Clostridia*
519 species from clusters IV of has consistently been shown leads to the increase of
520 regulatory T cells which secrete the anti-inflammatory cytokine IL-10 [52]. In line with
521 this, WRP supplementation led to enhanced *Clostridium* cluster IV enrichment, which
522 was positively related to butyrate in caecum and negatively related to TNF-α ($p < 0.05$)
523 and LPS ($p < 0.05$) (**Figure 8**) .

524 The most remarkable differences caused by WRP was in the Bacteroidetes phylum.
525 Consistently, we also found that WRP led to enhanced Bacteroidales abundance, which
526 was positively related to butyrate in caecum and gut index ($p < 0.05$), and negatively
527 correlated with the body weight gain, TC ($p < 0.01$), insulin ($p < 0.05$), and LPS levels
528 ($p < 0.01$). Furthermore, HFD caused by a decrease in the abundance of the
529 Porphyromonadaceae family and, in particular, the *Barnesiella* genus which has been
530 proved to positively impact on reducing the pro-inflammatory milieu in the gut [53]. Chiu
531 et al. has reported higher levels of *Barnesiella* in lean individuals compared to obese
532 patients [54]. These variables were consistently confirmed by us, WRP elevated the levels
533 of *Barnesiella* and Porphyromonadaceae which were negatively correlated with body
534 weight and TC ($p < 0.05$), positively correlated with gut index ($p < 0.05$). In contrast,

535 an increase in *Alistipes* genus of HFD-fed mice was observed in this study. Gram-
536 negative *Alistipes* was the foremost noteworthy taxon related to obesity and was found
537 to be expanded beneath HFD conditions [55].

538 In addition, we have also detected an enrichment of *Roseburia*. The *Roseburia*
539 (Actinobacteria phylum) was a typical SCFAs-producing bacterium within the intestine
540 that can anaerobically degrade polysaccharides such as arabinoxylan into SCFAs,
541 which protected against HFD-induced obesity by activating the release of gut hormone
542 and enhancing intestinal barrier function [45, 56]. Several reports pointed out that the
543 content of acetic acid and propionic acid were associated with an increased abundance
544 of *Olsenella* in pectin or fructo-oligosaccharides-fed mice [57-58]. However, As
545 highlighted by some researchers, *Olsenella* could be a target bacterial flora for obesity
546 since it was enriched considerably in HFD-fed mice [48, 59-60]. Based on our findings, the
547 abundance of *Olsenella* was enriched by HFD while it reduced to the level close to the
548 CD group after WRP supplementation. Our results exhibit high level of *Acetivibrio* in
549 HFD-WRP group and negatively correlated to body weight ($p < 0.01$), TC ($p < 0.05$).
550 Data published by Yang et al. shown maize-derived feruloylated polysaccharides
551 significantly increased *Acetivibrio* and controlled the weight gain induced by HFD [61].
552 One hypothesis is that multiple glycoside hydrolase secreted from *Acetivibrio*
553 hydrolyzed arabinose side chain of WRP and stimulated SCFAs production, as cecal
554 butyrate level positively correlated with *Acetivibrio* [62].

555 Previous research has illustrated that HFD triggered inflammatory responses,

556 defecting gut barrier integrity, and increasing the cytokines [55]. In our model, WRP
557 treatment significantly decreased the level of serum LPS and TNF-α in HFD-fed mice.
558 Specifically, the LPS-producing microbiota such as *Desulfovibrio* and *Mucispirillum*
559 became abundant after HFD feeding [48]. Notably, *Mucispirillum* has been described as
560 a mucus-associated bacterium that bursts during inflammation in HFD-induced obese
561 mouse model [63]. *Desulfovibrio* is one kind of genus belonging to Desulfovibrionaceae
562 and Proteobacteria, positively related to obesity-induced inflammation [64]. Moreover,
563 the correlation analysis further verified that the significant correlation between
564 *Desulfovibrio* and these obesity-related indexes (**Figure 8**).

565 On the other hand, butyrate and other short chain fatty acids are known to inhibit
566 fat accumulation and adipocyte dysfunction [65]. Here, we found that WRP intervention
567 significantly enriched the fecal and ceacal butyrate. Moreover, the correlation analysis
568 verified the positive association of microbiota diversity with ceacal butyrate. Several
569 studies reported that *Barnesiella*, *Roseburia*, *Clostridium* cluster IV, and *Butyrivibrio*
570 which are highly associated with the production of SCFAs, especially the synthesis of
571 butyrate [45]. Moreover, suppression HFD-induced body weight gain of WRP could
572 related to SCFAs secreted by relevant microbes (**Figure S2**). In line with this, it has
573 been revealed that WRP treatment enriched these microbes and prevented the HFD-
574 induced gut dysbiosis in mice.

575 Interestingly, a crucial analysis revealed that SCFAs can stimulated the white
576 adipose tissue browning [66]. Consistently, we also found WRP supplementation reduced

577 the white adipose tissue's weight, upregulated UCP1 expression, a specific protein
578 uncouples respiration from ATP synthesis and generates heat (**Figure 4**). Moreover,
579 WRP showed potential in fat browning by activating PGC-1α, a master regulator of
580 mitochondrial biogenesis [67]. Compared with the HFD group, gene expressions of the
581 beige adipocyte-selective markers including UCP1, TMEM26, CD137, and Cidea were
582 markedly increased in HFD-WRP group (**Figure 4B&C**). The above results indicated
583 that the supplementation of WRP triggered the browning of iWAT in HFD-fed mice.
584 Overall, we found that WRP can attenuate HFD-induced obesity, inflammation
585 and gut dysbiosis through combined effects of the white adipose browning and gut
586 microbiota modulation, while the CP (HG dominated pectin) and DWRP (less branched
587 RG-I oligosaccharide) have only limited effect on resistance to HFD-induced obesity.
588 Our findings convinced that highly branched RG-I domain enrichment are essential for
589 pectin mitigating against the HFD-induced obesity.
590591
591592
592 **Abbreviations**: BAT: Brown adipose tissue; CD: Normal chow diet; DWRP:
593 depolymerized fraction of RG-I enriched pectin from citrus segment membrane; HDL:
594 High density lipoprotein; HFD: High fat diet; OTU: Operational taxonomic units;
595 OGTT: Oral glucose tolerance test; PGC-1α: Peroxisome proliferators-activated
596 receptor-γ coactivator 1-alpha; RG-I: Rhamnogalacturonan-I; LDL: Low density
597 lipoprotein; LEfSe: Linear discriminant analysis effect size; TG: Total triacylglycerol;
598 TC: Total cholesterol; TNF-α: Tumor necrosis factor-α; UCP1: Uncoupling protein 1;

599 WAT: White adipose tissue; WRP: RG-I enriched pectin from citrus segment

600 membrane.

601 Acknowledgements

602 We thank Baokun Xie for his assistant to the graphs editing to this publication.

604

605 Ethics statement

606 The animal study was reviewed and approved by Zhejiang Chinese Medicine

607 University IACUC-20180917-02.

608 Funding

609 This work was financially supported in part by National Key R&D Program of 610

China (2017YFE0122300 190), National Natural Science Foundation of China

611 (3187181559) and Key R&D Program of Zhejiang Province (2020C02033)

612 **Author contributions**

613 S.G.C. conceived the study; K. Z. wrote the manuscript; G.Z.M. designed 614 experiments, performed the animal studies and statistical analysis; D.M.W. contributed 615 to sample preparation; C.X.Y. helped to perform the animal studies; H. X. helped to 616 revise the manuscript; X.Q.Y., R. J. L. and C.O. interpreted the data; S.G.C. critically

617 revised the manuscript. All authors read and approved the final manuscript. 618

Supporting information

619 The following are available online. Table S1: The compositions and energy 620 densities of the diets; Table S2: The specific formula of the high-fat diet; Table S3: 621 Diversity and richness of cecal microbiota in CP, WRP and DWRP supplements alter 622 the diversity; Table S4: The abundance of key phylotypes of gut microbiota in HFD-

623 fed C57BL/6J mice; Table S5: PCR primers used in this study; Figure S1: Weekly food

624 intake (A) and average food intake (B) of mice in response to dietary CP, WRP and 625

DWRP; Figure S2: LEfSe comparison of cecal microbiota. LDA score of cecal

626 microbiota between the CD, HFD, HFD-CP, HFD-WRP and HFD-DWRP groups.

627

628

629 **References**

630 1. Tagliabue, A.; Elli, M., The role of gut microbiota in human obesity: Recent 631 findings and future perspectives. *Nutrition, Metabolism and Cardiovascular Diseases* 632 **2013,** *23* (3), 160-168.

633 2. Zmora, N.; Suez, J.; Elinav, E., You are what you eat: diet, health and the gut 634 microbiota. *Nat Rev Gastroenterol Hepatol* **2019,** *16* (1), 35-56.

635 3. Stephens, R. W.; Arhire, L.; Covasa, M., Gut Microbiota: From 636 Microorganisms to Metabolic Organ Influencing Obesity. *Obesity* **2018,** *26* (5), 801-
637 809.

638 4. Bäckhed, F.; Ding, H.; Wang, T.; Hooper, L. V.; Koh, G. Y.; Nagy, A.; 639 Semenkovich, C. F.; Gordon, J. I., The gut microbiota as an environmental factor that 640 regulates fat storage. *Proceedings of the National Academy of Sciences of the United* 641 *States of America* **2004,** *101* (44), 15718-15723.

642 5. Ridaura, V. K.; Faith, J. J.; Rey, F. E.; Cheng, J.; Duncan, A. E.; Kau, A. L.; 643 Griffin, N. W.; Lombard, V.; Henrissat, B.; Bain, J. R.; Muehlbauer, M. J.; Ilkayeva, 644 O.; Semenkovich, C. F.; Funai, K.; Hayashi, D. K.; Lyle, B. J.; Martini, M. C.; Ursell, 645 L. K.; Clemente, J. C.; Van Treuren, W.; Walters, W. A.; Knight, R.; Newgard, C. B.; 646 Heath, A. C.; Gordon, J. I., Gut Microbiota from Twins Discordant for Obesity 647 Modulate Metabolism in Mice. *Science* **2013,** *341* (6150), 1241214-1241214.

648 6. Wu, T. R.; Lin, C. S.; Chang, C. J.; Lin, T. L.; Martel, J.; Ko, Y. F.; Ojcius, D. 649 M.; Lu, C. C.; Young, J. D.; Lai, H. C., Gut commensal *Parabacteroides goldsteinii* 650 plays a predominant role in the anti-obesity effects of polysaccharides isolated from 651 *Hirsutella sinensis*. *Gut* **2019,** *68* (2), 248-262.

652 7. Chang, C. J.; Lin, C. S.; Lu, C. C.; Martel, J.; Ko, Y. F.; Ojcius, D. M.; Tseng, 653 S. F.; Wu, T. R.; Chen, Y. Y.; Young, J. D.; Lai, H. C., *Ganoderma lucidum* reduces 654 obesity in mice by modulating the composition of the gut microbiota. *Nat Commun* 655 **2015,** *6*, 7489.

656 8. Liu, Y.; Chen, J.; Tan, Q.; Deng, X.; Tsai, P. J.; Chen, P. H.; Ye, M.; Guo, J.;
657 Su, Z., Nondigestible Oligosaccharides with Anti-Obesity Effects. *J Agric Food Chem*
658 **2020,** *68* (1), 4-16.

659 9. Palou, M.; Sanchez, J.; Garcia-Carrizo, F.; Palou, A.; Pico, C., Pectin

660 supplementation in rats mitigates age-related impairment in insulin and leptin 661 sensitivity independently of reducing food intake. *Mol Nutr Food Res* **2015,** *59* (10), 662 2022-33.

663 10. Hu, H.; Zhang, S.; Liu, F.; Zhang, P.; Muhammad, Z.; Pan, S., Role of the Gut 664 Microbiota and Their Metabolites in Modulating the Cholesterol-Lowering Effects of 665 Citrus Pectin Oligosaccharides in C57BL/6 Mice. *J Agric Food Chem* **2019,** *67* (43), 666 11922-11930.

667 11. Tingirikari, J. M. R., Microbiota-accessible pectic poly- and oligosaccharides 668 in gut health. *Food & Function* **2018,** *9* (10), 5059-5073.

669 12. Mao, G.; Wu, D.; Wei, C.; Tao, W.; Ye, X.; Linhardt, R. J.; Orfila, C.; Chen, 670 S., Reconsidering conventional and innovative methods for pectin extraction from fruit 671 and vegetable waste: Targeting rhamnogalacturonan I. *Trends in Food Science &* 672 *Technology* **2019,** *94*, 65-78.

673 13. Bang, S.-J.; Kim, G.; Lim, M. Y.; Song, E.-J.; Jung, D.-H.; Kum, J.-S.; Nam, 674 Y.-D.; Park, C.-S.; Seo, D.-H., The influence of in vitro pectin fermentation on the 675 human fecal microbiome. *AMB Express* **2018,** *8* (1), 98.

676 14. Karboune, S.; Khodaei, N., Structures, isolation and health-promoting 677 properties of pectic polysaccharides from cell wall-rich food by-products: a source of 678 functional ingredients. *Current Opinion in Food Science* **2016,** *8*, 50-55.

679 15. Patnode, M. L.; Beller, Z. W.; Han, N. D.; Cheng, J.; Peters, S. L.; Terrapon, 680 N.; Henrissat, B.; Le Gall, S.; Saulnier, L.; Hayashi, D. K.; Meynier, A.; Vinoy, S.; 681 Giannone, R. J.; Hettich, R. L.; Gordon, J. I., Interspecies Competition Impacts 682 Targeted Manipulation of Human Gut Bacteria by Fiber-Derived Glycans. *Cell* **2019,** 683 *179* (1), 59-73 e13.

684 16. Jiang, T.; Gao, X.; Wu, C.; Tian, F.; Lei, Q.; Bi, J.; Xie, B.; Wang, H.; Chen, 685 S.; Wang, X., Apple-Derived Pectin Modulates Gut Microbiota, Improves Gut Barrier 686 Function, and Attenuates Metabolic Endotoxemia in Rats with Diet-Induced Obesity. 687 *Nutrients* **2016,** *8* (3).

688 17. Licht, T. R.; Hansen, M.; Bergström, A.; Poulsen, M.; Krath, B. N.; 689 Markowski, J.; Dragsted, L. O.; Wilcks, A., Effects of apples and specific apple 690 components on the cecal environment of conventional rats: role of apple pectin. *BMC* 691 *Microbiology* **2010,** *10* (1), 13.

692 18. Luis, A. S.; Briggs, J.; Zhang, X.; Farnell, B.; Ndeh, D.; Labourel, A.; Baslé, 693 A.; Cartmell, A.; Terrapon, N.; Stott, K.; Lowe, E. C.; McLean, R.; Shearer, K.; 694 Schückel, J.; Venditto, I.; Ralet, M.-C.; Henrissat, B.; Martens, E. C.; Mosimann, S. C.; 695 Abbott, D. W.; Gilbert, H. J., Dietary pectic glycans are degraded by coordinated 696 enzyme pathways in human colonic Bacteroides. *Nature Microbiology* **2018,** *3* (2), 210-
697 219.

698 19. Martens, E. C.; Lowe, E. C.; Chiang, H.; Pudlo, N. A.; Wu, M.; McNulty, N. 699 P.; Abbott, D. W.; Henrissat, B.; Gilbert, H. J.; Bolam, D. N.; Gordon, J. I., Recognition 700 and degradation of plant cell wall polysaccharides by two human gut symbionts. *PLoS* 701 *Biol* **2011,** *9* (12), e1001221.

702 20. Larsen, N.; Bussolo de Souza, C.; Krych, L.; Barbosa Cahu, T.; Wiese, M.; 703 Kot, W.; Hansen, K. M.; Blennow, A.; Venema, K.; Jespersen, L., Potential of Pectins 704 to Beneficially Modulate the Gut Microbiota Depends on Their Structural Properties. 705 *Front Microbiol* **2019,** *10*, 223.
706 21. Luis, A. S.; Martens, E. C., Interrogating gut bacterial genomes for discovery 707 of novel carbohydrate degrading enzymes. *Current Opinion in Chemical Biology* **2018,** 708 *47*, 126-133.
709 22. Khodaei, N.; Fernandez, B.; Fliss, I.; Karboune, S., Digestibility and prebiotic 710 properties of potato rhamnogalacturonan I polysaccharide and its galactose-rich 711 oligosaccharides/oligomers. *Carbohydrate Polymers* **2016,** *136*, 1074-1084.
712 23. Bianchi, F.; Larsen, N.; de Mello Tieghi, T.; Adorno, M. A. T.; Kot, W.; Saad, 713 S. M. I.; Jespersen, L.; Sivieri, K., Modulation of gut microbiota from obese individuals 714 by in vitro fermentation of citrus pectin in combination with *Bifidobacterium longum* 715 BB-46. *Appl Microbiol Biotechnol* **2018,** *102* (20), 8827-8840.
716 24. Shinohara, K.; Ohashi, Y.; Kawasumi, K.; Terada, A.; Fujisawa, T., Effect of 717 apple intake on fecal microbiota and metabolites in humans. *Anaerobe* **2010,** *16* (5), 718 510-515.
719 25. Gullón, B.; Gómez, B.; Martínez-Sabajanes, M.; Yáñez, R.; Parajó, J. C.; 720 Alonso, J. L., Pectic oligosaccharides: Manufacture and functional properties. *Trends* 721 *in Food Science & Technology* **2013,** *30* (2), 153-161.
722 26. Gómez, B.; Gullón, B.; Yáñez, R.; Schols, H.; Alonso, J. L., Prebiotic potential 723 of pectins and pectic oligosaccharides derived from lemon peel wastes and sugar beet 724 pulp: A comparative evaluation. *Journal of Functional Foods* **2016,** *20*, 108-121.
725 27. Chen, J.; Liang, R.-h.; Liu, W.; Li, T.; Liu, C.-m.; Wu, S.-s.; Wang, Z.-j., 726 Pectic-oligosaccharides prepared by dynamic high-pressure microfluidization and their 727 in vitro fermentation properties. *Carbohydrate Polymers* **2013,** *91* (1), 175-182.
728 28. Centanni, M.; Carnachan, S. M.; Bell, T. J.; Daines, A. M.; Hinkley, S. F. R.; 729 Tannock, G. W.; Sims, I. M., Utilization of Complex Pectic Polysaccharides from New 730 Zealand Plants (*Tetragonia tetragonioides* and *Corynocarpus laevigatus*) by Gut 731 Bacteroides Species. *J Agric Food Chem* **2019,** *67* (27), 7755-7764.
732 29. Mao, G.; Li, S.; Orfila, C.; Shen, X.; Zhou, S.; Linhardt, R. J.; Ye, X.; Chen, 733 S., Depolymerized RG-I-enriched pectin from citrus segment membranes modulates 734 gut microbiota, increases SCFA production, and promotes the growth of 735 *Bifidobacterium spp.*, *Lactobacillus spp*. and *Faecalibaculum spp*. *Food & Function* 736 **2019,** *10* (12), 7828-7843.
737 30. Liu, Y.; Heath, A.-L.; Galland, B.; Rehrer, N.; Drummond, L.; Wu, X.-Y.; Bell, 738 T. J.; Lawley, B.; Sims, I. M.; Tannock, G. W., Substrate Use Prioritization by a 739 Coculture of Five Species of Gut Bacteria Fed Mixtures of Arabinoxylan, Xyloglucan, 740 β-Glucan, and Pectin. *Appl Environ Microbiol* **2020,** *86* (2), e01905-19.
741 31. Chen, J.; Cheng, H.; Wu, D.; Linhardt, R. J.; Zhi, Z.; Yan, L.; Chen, S.; Ye, 742 X., Green recovery of pectic polysaccharides from citrus canning processing water. 743 *Journal of Cleaner Production* **2017,** *144*, 459-469.

744 32. Fadrosh, D. W.; Ma, B.; Gajer, P.; Sengamalay, N.; Ott, S.; Brotman, R. M.; 745 Ravel, J., An improved dual-indexing approach for multiplexed 16S rRNA gene 746 sequencing on the Illumina MiSeq platform. *Microbiome* **2014,** *2* (1), 6.
747 33. Benjamini, Y.; Krieger, A. M.; Yekutieli, D., Adaptive linear step-up 748 procedures that control the false discovery rate. *Biometrika* **2006,** *93* (3), 491-507.
749 34. Canfora, E. E.; Jocken, J. W.; Blaak, E. E., Short-chain fatty acids in control 750 of body weight and insulin sensitivity. *Nat Rev Endocrinol* **2015,** *11* (10), 577-91.
751 35. Tanaka, H.; Kakiyama, T.; Takahara, K.; Yamauchi, M.; Tanaka, M.; Sasaki, 752 J.; Taniguchi, T.; Matsuo, H.; Shindo, M., The Association Among Fat Distribution, 753 Physical Fitness, and the Risk Factors of Cardiovascular Disease in Obese Women. 754 *Obesity Research* **1995,** *3* (S5), 649S-653S.
755 36. Odegaard, J. I.; Chawla, A., Pleiotropic Actions of Insulin Resistance and 756 Inflammation in Metabolic Homeostasis. *Science* **2013,** *339* (6116), 172-177.
757 37. Cani, P. D.; Amar, J.; Iglesias, M. A.; Poggi, M.; Knauf, C.; Bastelica, D.; 758 Neyrinck, A. M.; Fava, F.; Tuohy, K. M.; Chabo, C.; Waget, A.; Delmee, E.; Cousin, 759 B.; Sulpice, T.; Chamontin, B.; Ferrieres, J.; Tanti, J. F.; Gibson, G. R.; Casteilla, L.; 760 Delzenne, N. M.; Alessi, M. C.; Burcelin, R., Metabolic Endotoxemia Initiates Obesity 761 and Insulin Resistance. *Diabetes* **2007,** *56* (7), 1761-1772.
762 38. Weisberg, S. P.; McCann, D.; Desai, M.; Rosenbaum, M.; Leibel, R. L.; 763 Ferrante, A. W., Obesity is associated with macrophage accumulation in adipose tissue. 764 *Journal of Clinical Investigation* **2003,** *112* (12), 1796-1808.
765 39. Wang, W.; Seale, P., Control of brown and beige fat development. *Nature* 766 *Reviews Molecular Cell Biology* **2016,** *17* (11), 691-702.
767 40. Tilg, H.; Zmora, N.; Adolph, T. E.; Elinav, E., The intestinal microbiota 768 fuelling metabolic inflammation. *Nat Rev Immunol* **2020,** *20* (1), 40-54.
769 41. Mortensen, P. B.; Holtug, K.; Rasmussen, H. S., Short-Chain Fatty Acid 770 Production from Mono- and Disaccharides in a Fecal Incubation System: Implications 771 for Colonic Fermentation of Dietary Fiber in Humans. *The Journal of Nutrition* **1988,** 772 *118* (3), 321-325.
773 42. Li, S.; Li, M.; Yue, H.; Zhou, L.; Huang, L.; Du, Z.; Ding, K., Structural 774 elucidation of a pectic polysaccharide from *Fructus Mori* and its bioactivity on 775 intestinal bacteria strains. *Carbohydr Polym* **2018,** *186*, 168-175.
776 43. Onumpai, C.; Kolida, S.; Bonnin, E.; Rastall, R. A., Microbial utilization and 777 selectivity of pectin fractions with various structures. *Appl Environ Microbiol* **2011,** *77* 778 (16), 5747-5754.
779 44. Ndeh, D.; Gilbert, H. J., Biochemistry of complex glycan depolymerisation by 780 the human gut microbiota. *FEMS Microbiology Reviews* **2018,** *42* (2), 146-164.
781 45. Everard, A.; Lazarevic, V.; Gaia, N.; Johansson, M.; Stahlman, M.; Backhed, 782 F.; Delzenne, N. M.; Schrenzel, J.; Francois, P.; Cani, P. D., Microbiome of prebiotic- 783 treated mice reveals novel targets involved in host response during obesity. *ISME J* 784 **2014,** *8* (10), 2116-30.
785 46. Rosshart, S. P.; Vassallo, B. G.; Angeletti, D.; Hutchinson, D. S.; Morgan, A.

786 P.; Takeda, K.; Hickman, H. D.; McCulloch, J. A.; Badger, J. H.; Ajami, N. J.; 787 Trinchieri, G.; Pardo-Manuel de Villena, F.; Yewdell, J. W.; Rehermann, B., Wild 788 Mouse Gut Microbiota Promotes Host Fitness and Improves Disease Resistance. *Cell* 789 **2017,** *171* (5), 1015-1028.e13.
790 47. Zhao, Q.; Elson, C. O., Adaptive immune education by gut microbiota antigens. 791 *Immunology* **2018,** *154* (1), 28-37.
792 48. Li, S.; Li, J.; Mao, G.; Wu, T.; Hu, Y.; Ye, X.; Tian, D.; Linhardt, R. J.; Chen, 793 S., A fucoidan from sea cucumber Pearsonothuria graeffei with well-repeated structure 794 alleviates gut microbiota dysbiosis and metabolic syndromes in HFD-fed mice. *Food* 795 *Funct* **2018,** *9* (10), 5371-5380.
796 49. Pfeiffer, N.; Desmarchelier, C.; Blaut, M.; Daniel, H.; Haller, D.; Clavel, T., 797 *Acetatifactor muris* gen. nov., sp. nov., a novel bacterium isolated from the intestine of 798 an obese mouse. *Archives of Microbiology* **2012,** *194* (11), 901-907.
799 50. Biagi, E.; Nylund, L.; Candela, M.; Ostan, R.; Bucci, L.; Pini, E.; Nikkïla, J.; 800 Monti, D.; Satokari, R.; Franceschi, C.; Brigidi, P.; De Vos, W., Through Ageing, and 801 Beyond: Gut Microbiota and Inflammatory Status in Seniors and Centenarians. *PLOS* 802 *ONE* **2010,** *5* (5), e10667.
803 51. Reijnders, D.; Goossens, G. H.; Hermes, G. D.; Neis, E. P.; van der Beek, C. 804 M.; Most, J.; Holst, J. J.; Lenaerts, K.; Kootte, R. S.; Nieuwdorp, M.; Groen, A. K.; 805 Olde Damink, S. W.; Boekschoten, M. V.; Smidt, H.; Zoetendal, E. G.; Dejong, C. H.; 806 Blaak, E. E., Effects of Gut Microbiota Manipulation by Antibiotics on Host 807 Metabolism in Obese Humans: A Randomized Double-Blind Placebo-Controlled Trial. 808 *Cell Metab* **2016,** *24* (1), 63-74.
809 52. Cox, L. M.; Blaser, M. J., Antibiotics in early life and obesity. *Nat Rev* 810 *Endocrinol* **2015,** *11* (3), 182-90.
811 53. Arias, L.; Goig, G. A.; Cardona, P.; Torres-Puente, M.; Diaz, J.; Rosales, Y.; 812 Garcia, E.; Tapia, G.; Comas, I.; Vilaplana, C.; Cardona, P. J., Influence of Gut 813 Microbiota on Progression to Tuberculosis Generated by High Fat Diet-Induced 814 Obesity in C3HeB/FeJ Mice. *Front Immunol* **2019,** *10*, 2464.
815 54. Chiu, C.-M.; Huang, W.-C.; Weng, S.-L.; Tseng, H.-C.; Liang, C.; Wang, W.- 816 C.; Yang, T.; Yang, T.-L.; Weng, C.-T.; Chang, T.-H.; Huang, H.-D., Systematic 817 analysis of the association between gut flora and obesity through high-throughput 818 sequencing and bioinformatics approaches. *Biomed Res Int* **2014,** *2014*, 906168- 819 906168.
820 55. Dalby, M. J.; Ross, A. W.; Walker, A. W.; Morgan, P. J., Dietary Uncoupling 821 of Gut Microbiota and Energy Harvesting from Obesity and Glucose Tolerance in Mice. 822 *Cell Rep* **2017,** *21* (6), 1521-1533.
823 56. Zhang, C.; Abdulaziz Abbod Abdo, A.; Kaddour, B.; Wu, Q.; Xin, L.; Li, X.; 824 Fan, G.; Teng, C., Xylan-oligosaccharides ameliorate high fat diet induced obesity and 825 glucose intolerance and modulate plasma lipid profile and gut microbiota in mice. 826 *Journal of Functional Foods* **2020,** *64*.
827 57. Li, W.; Zhang, K.; Yang, H., Pectin Alleviates High Fat (Lard) Diet-Induced

828 Nonalcoholic Fatty Liver Disease in Mice: Possible Role of Short-Chain Fatty Acids 829 and Gut Microbiota Regulated by Pectin. *Journal of Agricultural and Food Chemistry* 830 **2018,** *66* (30), 8015-8025.

831 58. Mao, B.; Li, D.; Zhao, J.; Liu, X.; Gu, Z.; Chen, Y. Q.; Zhang, H.; Chen, W., 832 Metagenomic Insights into the Effects of Fructo-oligosaccharides (FOS) on the 833 Composition of Fecal Microbiota in Mice. *Journal of Agricultural and Food Chemistry* 834 **2015,** *63* (3), 856-863.

835 59. Kong, C.; Gao, R.; Yan, X.; Huang, L.; Qin, H., Probiotics improve gut 836 microbiota dysbiosis in obese mice fed a high-fat or high-sucrose diet. *Nutrition* **2019,** 837 *60*, 175-184.

838 60. Tang, D.; Wang, Y.; Kang, W.; Zhou, J.; Dong, R.; Feng, Q., Chitosan 839 attenuates obesity by modifying the intestinal microbiota and increasing serum leptin 840 levels in mice. *Journal of Functional Foods* **2020,** *64*.

841 61. Yang, J.; Bindels, L. B.; Segura Munoz, R. R.; Martinez, I.; Walter, J.; Ramer-842 Tait, A. E.; Rose, D. J., Disparate Metabolic Responses in Mice Fed a High-Fat Diet 843 Supplemented with Maize-Derived Non-Digestible Feruloylated Oligo- and 844 Polysaccharides Are Linked to Changes in the Gut Microbiota. *PLoS One* **2016,** *11* (1), 845 e0146144.

846 62. Cui, J.; Mai, G.; Wang, Z.; Liu, Q.; Zhou, Y.; Ma, Y.; Liu, C., Metagenomic 847 Insights Into a Cellulose-Rich Niche Reveal Microbial Cooperation in Cellulose 848 Degradation. *Front Microbiol* **2019,** *10*, 618.

849 63. Loy, A.; Pfann, C.; Steinberger, M.; Hanson, B.; Herp, S.; Brugiroux, S.; 850 Gomes Neto, J. C.; Boekschoten, M. V.; Schwab, C.; Urich, T.; Ramer-Tait, A. E.; 851 Rattei, T.; Stecher, B.; Berry, D., Lifestyle and Horizontal Gene Transfer-Mediated 852 Evolution of Mucispirillum schaedleri, a Core Member of the Murine Gut Microbiota. 853 *mSystems* **2017,** *2* (1), e00171-16.

854 64. Lennon, G.; Balfe, Á.; Bambury, N.; Lavelle, A.; Maguire, A.; Docherty, N. 855 G.; Coffey, J. C.; Winter, D. C.; Sheahan, K.; O'Connell, P. R., Correlations between 856 colonic crypt mucin chemotype, inflammatory grade and Desulfovibrio species in 857 ulcerative colitis. *Colorectal Disease* **2014,** *16* (5), O161-O169.

858 65. Kolodziejczyk, A. A.; Zheng, D.; Elinav, E., Diet-microbiota interactions and 859 personalized nutrition. *Nat Rev Microbiol* **2019,** *17* (12), 742-753.

860 66. Li, G.; Xie, C.; Lu, S.; Nichols, R. G.; Tian, Y.; Li, L.; Patel, D.; Ma, Y.; 861 Brocker, C. N.; Yan, T.; Krausz, K. W.; Xiang, R.; Gavrilova, O.; Patterson, A. D.; 862 Gonzalez, F. J., Intermittent Fasting Promotes White Adipose Browning and Decreases 863 Obesity by Shaping the Gut Microbiota. *Cell Metabolism* **2017,** *26* (4), 672-685.e4.

864 67. Seale, P., Transcriptional Regulatory Circuits Controlling Brown Fat 865 Development and Activation. *Diabetes* **2015,** *64* (7), 2369-2375.

866

867

868 **Tables**

869

870

871 **Table 1** Effects of RG-I pectin on serum biochemical parameters in C57BL/6 Mice

872

Groups	CD	HFD	HFD-CP	HFD-WRP	HFD-DWRP
TC (mmol/L)	4.99±0.65 [a]	9.66±0.75 [d]	8.58±0.76 [c]	5.28±0.42 [a]	6.43±0.56 [b]
TG (mmol/L)	1.15±0.27 [a]	1.49±0.11 [b]	1.41±0.21 [ab]	1.26±0.30 [ab]	1.27±0.15 [ab]
HDL-C (mmol/L)	1.52±0.27 [a]	2.10±0.37 [ab]	2.12±1.02 [bc]	2.65±0.62 [c]	2.81±1.47 [c]
LDL-C (mmol/L)	1.99±0.45 [a]	4.00±1.78 [b]	2.94±0.39 [a]	2.01±0.54 [a]	2.29±0.77 [a]
FFA (mmol/L)	1.27±0.43 [ab]	1.72±0.12 [b]	1.57±0.47 [b]	1.33±0.33 [ab]	1.20±0.44 [a]
Insulin (ng/mL)	0.38±0.12 [a]	0.76±0.27 [c]	0.61±0.19 [bc]	0.50±0.20 [ab]	0.56±0.15 [ab]
LPS (EU/mL)	0.44±0.02 [ab]	0.54±0.05 [c]	0.54±0.14 [bc]	0.41±0.07 [a]	0.39±0.07 [a]
TNF-α (ng/mL)	1.29±0.55 [bc]	1.58±0.35 [c]	0.91±0.39 [ab]	0.68±0.19 [ab]	0.52±0.12 [a]
Adiponectin (ug/mL)	51.03±12.95 [d]	27.14±3.62 [a]	31.52±3.54 [ab]	47.77±9.45 [cd]	38.07±4.36 [bc]
TG/HDL-C	0.74±0.24 [a]	0.75±0.14 [a]	1.33±1.25 [a]	0.48±0.05 [a]	0.55±0.19 [a]
HDL-C/LDL-C	0.78±0.11 [a]	0.57±0.22 [a]	0.63±0.33 [a]	1.38±0.43 [b]	1.54±1.19 [b]

873 The means with different superscript letters (a, b, and c) represent statistically significant results (p 874 < 0.05) based on one-way analysis of variance (ANOVA) with Duncan's range tests, whereas means 875 labeled with the same superscript correspond to results that show no statistically significant 876 differences.

877

878

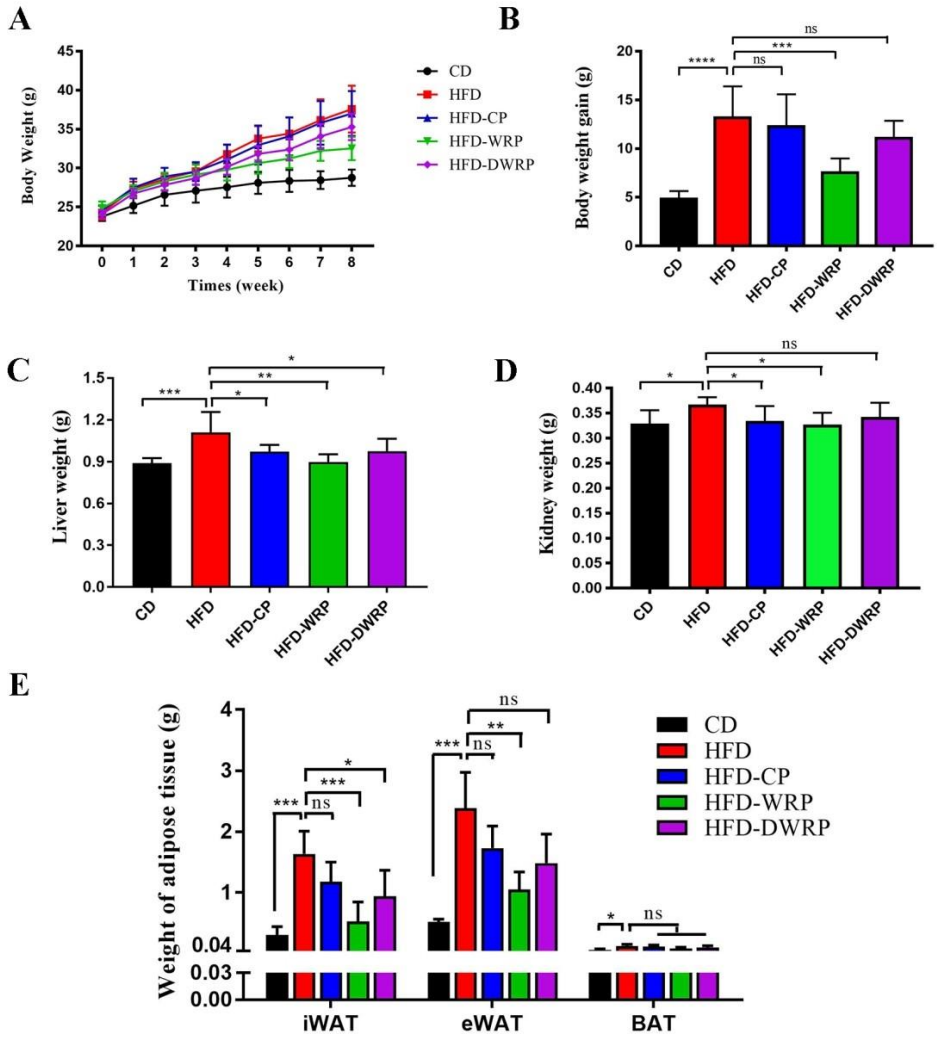
A
Body Weight (g)
Times (week)
CD
HFD
HFD-CP
HFD-WRP
HFD-DWRP
B
Body weight gain (g)
C
Liver weight (g)
D
Kidney weight (g)
E
Weight of adipose tissue (g)
iWAT
eWAT
BAT

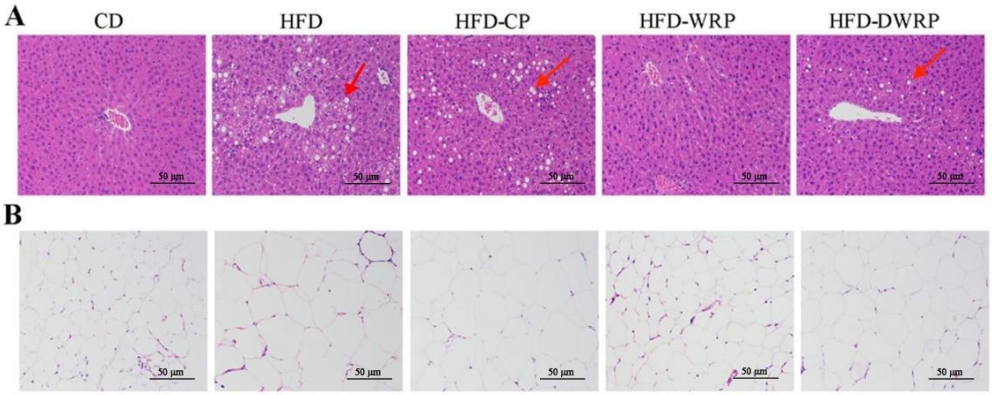

Figure 2. Histological assessment of livers (A) and epididymal white adipose tissue (B) in HFD-induced obesity mice (H&E stain, 200□magnification)

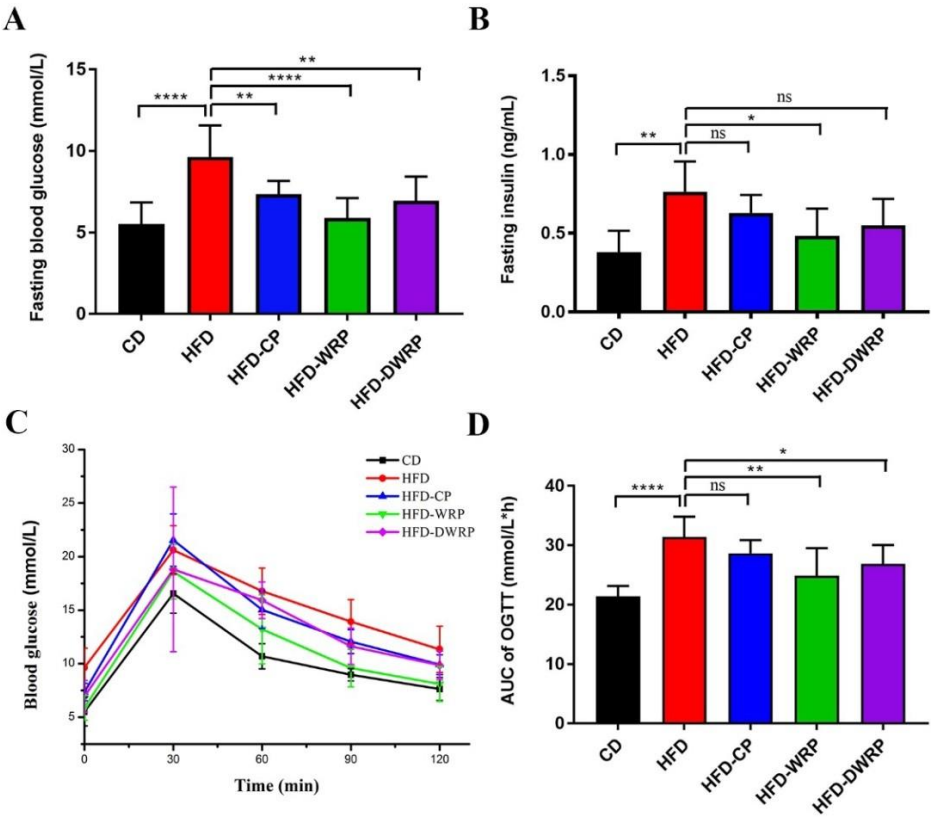
A
Fasting blood glucose (mmol/L)
15
10
5
0
****
**
****
**
CD
HFD
HFD-CP
HFD-WRP
HFD-DWRP
B
Fasting insulin (ng/mL)
1.5
1.0
0.5
0.0
**
ns
*
ns
CD
HFD
HFD-CP
HFD-WRP
HFD-DWRP
C
Blood glucose (mmol/L)
30
25
20
15
10
5
0
30
60
90
120
Time (min)
CD
HFD
HFD-CP
HFD-WRP
HFD-DWRP
D
AUC of OGTT (mmol/L*h)
40
30
20
10
0
****
ns
**
*
CD
HFD
HFD-CP
HFD-WRP
HFD-DWRP

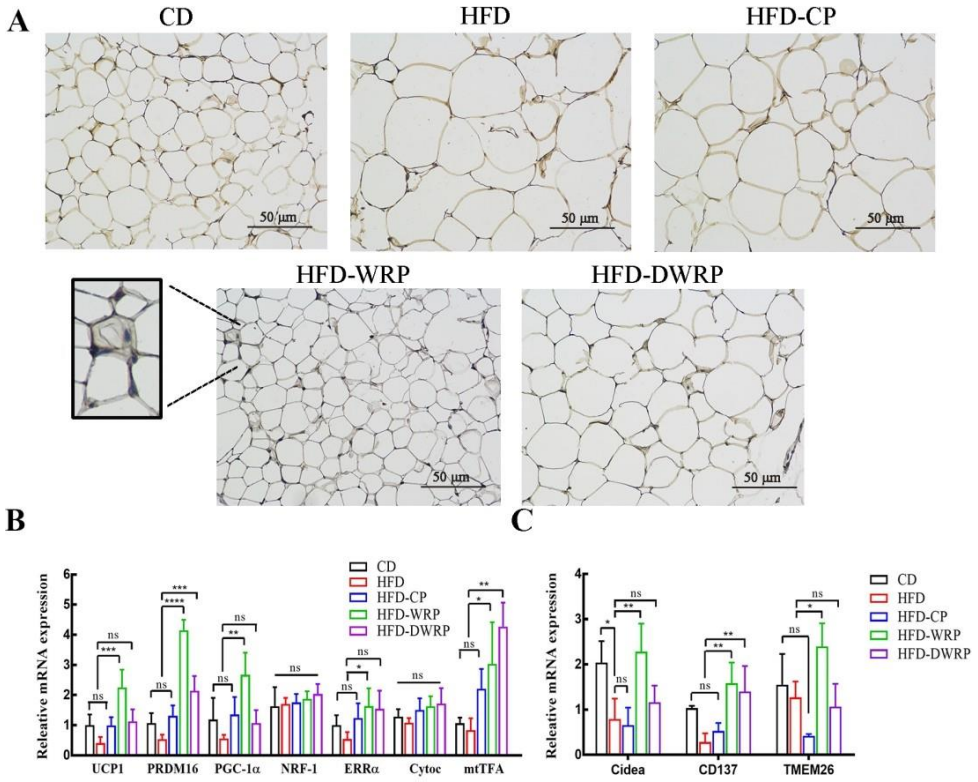

Figure 4. RG-I enriched pectin promoted thermogenesis and browning in iWAT of HFD-fed C57BL/6J mice. (A) Immunohistochemistry for UCP1 protein in iWAT of HFD-fed C57BL/6J mice (magnification 200 times). (B) Thermogenic genes and (C) beige adipocyte-selective markers in iWAT. Relative expression of UCP1, PRDM16, PGC-1α, Nuclear respiratory factor-1 (NRF-1), estrogen-related receptor α (ERRα), Cytochrome c (Cytoc), mitochondrial transcription factor A (mtTFA), Cidea, CD137 and TMEM26 was assessed by qRT-PCR and was Compared to the HFD group. Results are expressed as mean± SD (n≥5). ns, not significant,; (*)(**)(***)p＜0.05, 0.01, 0.001, Compared to the HFD group based on one-way analysis of variance (ANOVA) with Duncan's range tests

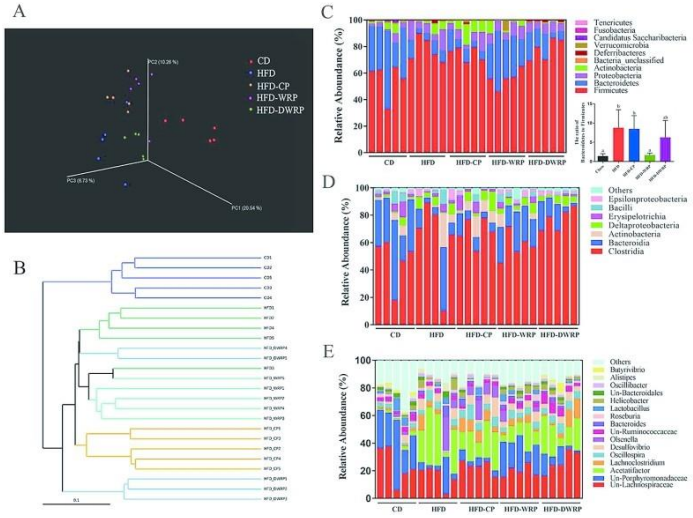

Figure 5. Structural composition of gut microbiota. (A) PCoA plot of cecal microbiota in HFD-fed mice based on weighted UniFrac metric. (B) UPGMA analysis of cecal microbiota of HFD-fed mice. Cecal microbiota in CD, HFD, HFD-CP, HFD-WRP and HFD-DWRP groups at phylum (C), class (D) and genus (E) level

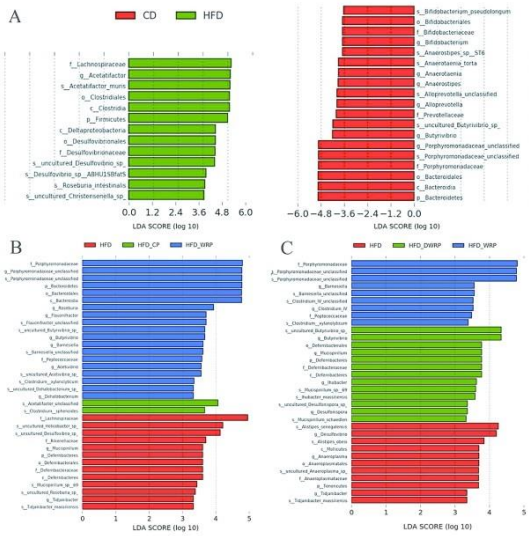

Figure 6. LEfSe comparison of gut microbiota. (A) The LDA score between CD and HFD groups, with LDA score > ±3.6; (B) The LDA score between CD、HFD-WRP and HFD-CP groups, with LDA score＞3.3; (C) The LDA score between CD、HFD-WRP and HFD-DWRP groups, with LDA score＞3.3.

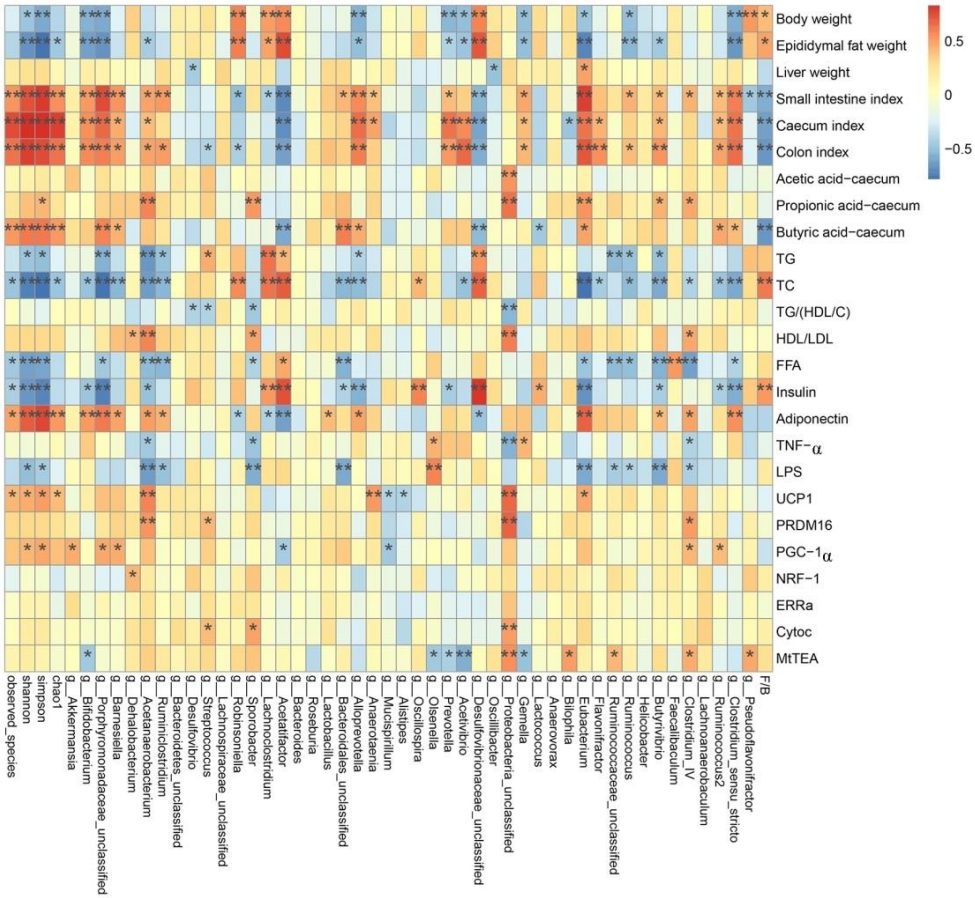

Figure 7. Heatmap of Sperman's correlation between cecal microbiota and health-related indexes. The indexes of α diversity including observed species; the Shannon, Simpson, and Chao1 indexes; The colors range from blue (negative correlation) to red (positive correlation). Significant correlations are marked by *p < 0.05 and **p < 0.01